NUMERICAL MODELING OF SOUND TRANSMISSION CHARACTERISTICS THROUGH A SEMI-CYLINDRICAL PANEL

BY

LIKHON BISWAS

CLASS ROLL NO: 001410402020

EXAM ROLL NO: M4CIV1610

REGN. NO: 104127 of 2008-09

UNDER THE GUIDANCE OF

PROF. PARTHA BHATTACHARYA

A Thesis be submitted

In Partial Fulfillment 0f the Requirements for the Degree of

MASTER OF ENGINEERING IN CIVIL ENGINEERING

(SPECIALIZATION: *STRUCTURAL ENGINEERING*)

IN THE

DEPARTMENT OF CIVIL ENGINEERING

FACULTY OF ENGINEERING AND TECHNOLOGY

JADAVPUR UNIVERSITY

KOLKATA – 700 032 INDIA

MAY, 2016

CERTIFICATE OF RECOMMENDATION

This is to certify that **Likhon Biswas** (Class Roll No.- 001410402020, Examination Roll No. - M4CIV1610, Registration No. - 104127 of 2008-09) has carried out the thesis work entitled, "**NUMERICAL MODELING OF SOUND TRANSMISSION CHARACTERISTICS THROUGH A SEMI-CYLINDRICAL PANEL**", under my direct supervision & guidance. He carried out this work independently. I hereby recommend that the thesis be accepted in partial fulfillment of the requirements for awarding the degree of "**MASTER OF ENGINEERING IN CIVIL ENGINEERING (STRUCTURAL ENGINEEERING)**"

…….

DR. PARTHA BHATTACHARYA

Professor Department of Civil Engineering
Jadavpur University
Kolkata-700 032

Date:……

Countersigned by....

……..

Dean
(Prof. Dr. Sivaji Bandyopadhyay)
Faculty of Engineering and Technology
Jadavpur University
Kolkata-700 032
Date:.....

……

Head of the Department
(Prof. Dr. R. B. Sahu)
Department of Civil Engineering
Jadavpur University
Kolkata-700032
Date:.....

CERTIFICATE OF APPROVAL

This foregoing thesis is hereby approved as a credible study on an Engineering subject carried out and presented in a manner satisfactory to warrant its acceptance as a prerequisite to the degree for which it has been submitted. It is understood that by this approval the undersigned do not necessarily endorse or approve any statement made, opinion expressed or conclusion drawn therein, but approve the thesis only for the purpose for which it is submitted.

Committee on final examination for evaluation of the thesis.

……

.....

……..

(Signature of the Examiners)

DECLARATION

I, Likhon Biswas, a student of Master of Engineering in Civil Engineering (Structural Engineering), Jadavpur University, Faculty of Engineering & Technology, hereby declare that the work being presented in the thesis work entitled, "**Numerical Modeling of Sound Transmission Characteristics through a Semi-Cylindrical Panel**", is authentic record of work that has been carried out at the Department of Civil Engineering, Jadavpur University, under the guidance of Dr. Partha Bhattacharya, Professor, Department of Civil Engineering, Jadavpur University.

The work contained in the thesis has not yet been submitted in part or full to any other university or institution or professional body for award of any degree or diploma or any fellowship.

Date:..... …….

Place: Jadavpur University, Kolkata

(LIKHON BISWAS)
Class Roll no.- 001410402020
Registration no. - 104127 of 2008-2009
Exam Roll no.:- M4CIV1610
Jadavpur University

ACKNOWLEDGEMENTS

I would like to express my sincere gratitude and thanks to my guide, Dr Partha Bhattacharya, for his guidance, constant encouragement and support during the course of my work in the last one year. I truly appreciate and value his esteemed guidance and encouragement from the beginning to the end of the thesis. His knowledge and company at the time of crises would be remembered lifelong.

Very special thanks to my mother for her continuous support during the entire course of my thesis work.

I must admit and appreciate the help and support received from my senior fellow researchers, Mr. Atanu Sahu, Mr. Biplab Ranjan Adikari, Mr. Sougata Das and my friends, Falguni, Subhankar, Bibekananda, Sourav. My special thanks to Subhadip and Rairupa continuous encouragement and support throughout the work.

I would also like to offer my sincere thanks to all faculty members, teaching and non-teaching staff of Civil Engineering Department of Jadavpur University for their assistance.

Date:.....

Place: Jadavpur University, Kolkata

…….

(LIKHON BISWAS)

ABSTRACT

Semi-cylindrical curved structures are used in many engineering applications, i.e. aircraft engineering. Estimation of sound transmission through the wall of aircraft structures is a major concern in modern time. Several research works were performed in the past few decades to understand the sound transmission behavior through the panel of the vibro-acoustic system. Most of the works deals with flat structures while only a few with curved structure. However a suitable vibro-acoustic model for sound transmission through a semi-cylindrical curved structure is yet to be developed. In this quest, the present work tries to delve into the modeling of energy transmission through a semi-cylindrical single wall and also a semi-cylindrical double wall. Subsequently,energy transmission parameters are studied in the low frequency range for various parameters of the model, such as different types of load, there orientation and point of application, different damping coefficients, different material properties etc. A model expansion theory based on Green's theorem is implemented to model the energy transmission through as acoustically coupled semi-cylindrical single wall panel and also double wall panel. The developed model is first validated with numerical models available.It has been observed in the present study that the structure dominates the energy transmission in single wall model. In low frequency region the performance of isotropic (aluminum) material is better than laminated composite materials in reduction of energy transmission of coupled system.

LIST OF SYMBOLS

Symbol	Description
c_0	velocity of sound in the air
c_e	velocity of sound in enclosure
c_g	velocity of sound in the gap cavity
d_n	amplitude of modal pressure of the enclosure at mode n
$\tilde{F}(x, y, z, t)$	External force on panel ‘a’
F_0	amplitude of harmonic forcing
F_a	generalized force applied to the panel ‘a’
H_{11}	Modal dynamic stiffness of curved panel ‘a’
H_{13}	Coupling coefficients representing the effect of acoustic pressure of the gap cavity on the structural response on panel ‘a’
H_{22}	Modal dynamic stiffness of curved panel ‘b
H_{23}	Coupling coefficients representing the effect of acoustic pressure of the gap cavity on the structural response on panel ‘b’
H_{24}	Coupling coefficients representing the effect of acoustic pressure of the enclosure on the structural response on panel ‘b’
H_{31}	Coupling coefficients representing the effect of the structural vibration of panel ‘a’ on the cavity pressure
H_{32}	Coupling coefficients representing the effect of the structural vibration of panel ‘b’ on the cavity pressure
H_{33}	Modal dynamic stiffness of the gap cavity
H_{42}	Coupling coefficients representing the effect of the structural vibration of panel ‘b’ on the enclosure pressure
H_{44}	Modal dynamic stiffness of the enclosure
i	complex quantity = $\sqrt{-1}$

LIST OF SYMBOLS (continued)

Symbol	Description
K	acoustic wavenumber = ω/c_0
K_a	Stiffness of panel 'a'
K_b	Stiffness of panel 'b'
$L_{l,j}^{ag}$	modal coupling coefficient between the acoustical mode l of the gap cavity and the structural mode j of panel 'a'
$L_{l,k}^{bg}$	modal coupling coefficient between the acoustical mode l of the gap cavity and the structural mode k of panel 'b'
$L_{n,k}^{be}$	modal coupling coefficient between the acoustical mode n of the enclosure and the structural mode k of panel 'b'
$L_{p,g}$	Averaged sound pressure level of the gap cavity
$L_{p,e}$	Averaged sound pressure level of the enclosure
M_a	Mass of panel 'a'
$m_{a,j}$	generalized mass of panel 'a' at mode j
M_b	Mass of panel 'b'
$m_{b,k}$	generalized mass of panel 'b' at mode k
$m_{e,n}$	Generalized mass of the enclosure at mode n
$m_{g,l}$	generalized mass of the gap cavity at mode l
M_{jl}	monopole coefficient relating velocity at l^{th} element to pressure at j^{th} element
n_g	normal direction directed outwards from air gap boundary
$\mathbf{n_e}$	normal direction directed outwards from enclosure boundary
nma	total no of modes taken into account for the panel 'a'

LIST OF SYMBOLS (continued)

Symbol	Description
nmb	total no of modes taken into account for the panel 'b'
nme	total no of modes taken into account for the enclosure
nmg	total no of modes taken into account for the gap cavity
$\widetilde{P}(\omega)$	total radiated sound power
$\tilde{p}(\mathbf{r}, \omega)$	amplitude of the acoustic pressure at an angular frequency ω at **r**
$P_e(x, y, z, t)$	acoustic pressure in the enclosure
$P_{eb}(x, y, z, t)$	acoustic pressure of the enclosure on panel 'b'
$p_{e,n}(t)$	modal pressure of the enclosure at mode n
$P_g(x, y, z, t)$	Acoustic pressure in the air gap
$P_{ga}(x, y, z, t)$	acoustic pressure of the gap cavity on panel 'a'
$P_{gb}(x, y, z, t)$	acoustic pressure of the air gap on panel 'b'
$p_{g,l}(t)$	modal pressure of the air gap at mode l
S_a	Surface area of panel 'a'
S_b	Surface area of panel 'b'
s_l	elemental area
V_e	Volume of the enclosure
V_g	Volume of the gap cavity
v_j^H	complex conjugate of the velocity over the element
$\langle \mathbf{V^2} \rangle$	Averaged quadratic velocity
w_a	normal component of the structural displacements of panel 'a'
w_b	normal component of the structural displacements of panel 'b'

LIST OF SYMBOLS (continued)

Symbol	Description
$x_a(x, y, z, t)$	Displacement function of panel ‘a’
$x_b(x, y, z, t)$	Displacement function of panel ‘b’
$\zeta_{a,j}$	modal loss factor of panel ‘a’ at mode j
$\zeta_{b,k}$	modal loss factor of panel ‘b’ at mode k
$\zeta_{e,n}$	modal loss factor of the enclosure at mode n
$\zeta_{g,l}$	modal loss factor of the air gap at mode l
ω	Excitation frequency
$\omega_{a,j}$	natural frequency of panel ‘a’ at mode j
$\omega_{b,k}$	natural frequency of panel ‘b’ at mode k
$\omega_{e,n}$	natural frequency of the enclosure at mode n
$\omega_{g,l}$	natural frequency of the air gap at mode l
$\varphi_{a,j}(x, y, z)$	Mode shape function of panel ‘a’ at mode j
$\varphi_{b,k}(x, y, z)$	Mode shape function of panel ‘b’ at mode k
$\varphi_{e,n}(x, y, z)$	mode shape function of the enclosure at mode n
$\varphi_{g,l}(x, y, z)$	mode shape function of the air gap at mode l
ρ	density of the surrounding fluid medium
ρ_g	equilibrium fluid density of gap cavity
ρ_e	equilibrium fluid density of enclosure
$\psi_{a,j}$	normal mode shape of panel ‘a’ at mode j
$\psi_{b,k}$	normal mode shape of panel ‘b’ at mode k

CONTENTS

LIST OF FIGURES

LIST OF TABLES

CHAPTER 1: INTRODUCTION

1.1. Background and Motivation

Sound may be expressed as the time-dependent change of the density of the fluid and associated time-dependent pressure fluctuation around the mean static pressure. For example, when a tuning fork vibrates, the vibration of the elastic structure generates a pressure fluctuation in air, which is heard as sound. There are many sources of sound such as produced by a disturbed flow or by the vibration of structures. Among them, sound generated from a vibrating structure is frequently encountered in real life. The field of study which combines the vibration of structures and acoustic wave propagation through a surrounding fluid medium is termed as **vibro-acoustics or structural acoustics**. Vibro-acoustics basically deals with the interaction of sound with the structure which is associated with an exchange of vibrational and acoustic energy. Aerospace, automotive vehicle structures, buildings are some of the examples where the external disturbance on the structures causes the structure to vibrate and the increase in interior acoustic pressure is the effect of the same.

Excessive unwanted sound, which is often referred to as noise, has sometimes serious adverse effects on human beings. It may cause permanent or partial hearing damage or exposure to unwanted sound may rise the stress level, which ultimately results cardiac hypertension, stroke, depression, etc. Apart from the human health problems, excessive sound poses a serious threat to mechanical systems such as aircraft structures, space rockets, etc. inflicting serious fatigue damage. To avoid health problems, environmental pollution (noise pollution), structural damage of vehicles, modeling and estimation of generated noise and its mitigation has become a major challenge to the modern civilization.

In vibro-acoustic problems, a no slip condition at the interface between a structure and the surrounding fluid is assumed in the direction normal to the solid structural surface. Therefore, a mutual coupling exists between the acoustic medium and the vibrating structure by virtue of which the vibration of the structure is transmitted to the acoustic domain as sound and sound from the fluid medium transforms to the structural vibration. Therefore a coupled structural acoustic analysis is required to predict the system behaviour.

The sound transmission through any partition can be broadly classified into two classes – (a) transmission into a free space and (b) transmission into closed space. Although the transmission phenomenon is very similar in both the cases, the treatment of the problem is significantly different. This is due to the fact that in interior acoustics, standing waves are created which are not there in free field acoustic problems. Due to this fact, for sound transmission into closed cavity, the interaction between the acoustic cavity modes and the structural modes assumes special significance. In the present study an interior acoustics problem is considered, such as sound transmission into an aircraft fuselage or into an enclosed cabin.

To assess the sound quality of a product or noise transmission characteristics, efficient numerical and experimental tools are needed. However, it is always expensive to conduct an experiment every time on a prototype. Thus, numerical analysis started gaining popularity and it is required to predict the noise level with a reasonable accuracy, quickly and with necessary spatial resolution. One of the most common numerical analysis to understand sound transmission characteristics is the finite element method. There are few more techniques available in literature like boundary element method (BEM), statistical energy analysis (SEA), hybrid approach etc. Among them SEA is mostly used for analysis in high frequency regime, hybrid approach effective for used for analysis in mid frequency zones, whereas in low frequency coupled problems the FEM and BEM are popular. In the present thesis, a coupled vibro-acoustic model is developed based on the FEM technique to study the sound transmission characteristics.

Modern day aircrafts are built with lightweight structural systems for fuel efficiency which is, however, inherently very poor at reducing the sound transmission from external sources. Hence, it is very important to address the problem of sound transmission and reduction of the same during the design stage itself. A clear understanding of the energy transfer mechanism through the vehicular wall is of paramount importance in the design of such a structure. Not only aircraft, this study is also important for noise control inside an automobile cabin, watercraft, auditorium, and control rooms.

It is a well-known fact that for an aircraft or automobile, the major source of noise is the engine that contributes to both mechanical and acoustic noise sources. The exterior perturbations on the fuselage skin and airframe are transmitted as airborne and structure-borne noise on the trim panel and form the primary source of interior noise. Extensive research over the years resulted in quieter engines and better suspension system that has made modern aircraft interiors an improved place in terms of acoustic disturbance. In the last few decades research is going on, to optimize the fuselage sidewalls with respect to their sound transmission capability by adopting various single wall models, or various double wall model or addition of sound proofing materials etc., which have resulted in satisfactory noise pressure level reduction in the cabin. In the present study, some single wall and double well model are developed to understand the sound transmission behaviour.

However, it is observed that the addition of sound proofing material on the fuselage walls does not efficiently increase the transmission loss below 500 Hz. It has been observed by Kaczmarska and Augustynska (1992) that the sound insulation ability of “soundproof’ cabins averages typically 30-50 dB for frequencies above 500 Hz, but only 0 – 19 dB for frequencies below 500 Hz. Depending on the flight condition, various tonal and broadband noise components in this frequency range (De Fonseca et al. [1]), especially due to buzz-saw noise and jet noise emitted by the engines and the turbulent boundary layer along the fuselage, are still perceived as very annoying by passengers. Thus, passenger comfort could further be improved by decreasing the structural sound transmission into the cabin at lower audible frequencies. However, the low frequency sound transmission is mainly controlled by the area weight of the structure and a substantial decrease in sound transmission would

require an important increase in mass, hence representing a non-viable option for aircraft interior noise control. In the present study the frequency zone is kept limited up to 500 Hz.

In case of sound transmission through single wall, several research articles show that the sound reduction index at a given frequency increases 5-6 dB per doubling the mass provided that no coincidence transmission occurs. But in many applications there exists mass constraint from the requirement of lightweight structure. Especially in case of modern fuel efficient aerospace vehicle or automobile vehicle, the structure is kept very lightweight.

In this quest, it is worth mentioning that the double wall structures are widely used in many engineering applications due to their superior thermal and acoustic insulation characteristics. Typical examples of double wall structures include double-glazed windows, gypsum office partitions or aircraft fuselages. Double wall structure is composed of two structural panels separated by a gap. The intermediate gap may be either filled up with air or can have glass wool or any kind of sound proofing materials. In certain cases there may exist mechanical connection between two panels. Mechanical connection creates mechanical transmission path for sound transmission from one panel to another beside acoustic transfer path.

A furthermore improvement in this field is double-wall curved surface consisting of two concentric shell surface separated by an air gap. In aerospace, marine and other engineering applications, cylindrical shells often occur as a part of the double wall curved surface construction for the purpose of noise insulation, streamlining requirements, thermal shield or interior finish requirements. For an aerospace fuselage structure, the outer shell represents exterior skin whereas the inner shell represents the trim panel. The outer shell is also stiffened by longitudinal stiffeners and transverse stiffeners in aircraft fuselage structure. In case of structures highlighted in above discussion, interior portion or enclosure also plays a significance role in acoustic transmission. The interaction between the acoustic cavity modes and structural modes assumes special significance.

From these viewpoints, the present work delves into the formulation of energy transmission through a double-wall curved panel consisting of two cylindrical shell panels separated by an air gap. The simple analogy for a double panel is that the system can be represented by two masses on the ends of a spring. The air space may be considered to behave as a simple spring if the wavelength of the sound is much greater than the spacing between the panels a condition which clearly applies when it is recalled that the wavelengths range from 11 ft. at 100 Hz down to 3 in at 4,000 Hz, i.e. over the frequency band wherein the present problems arise. Vibration set up in one mass may be transferred by the spring to the other mass, often with little diminution at most of the frequencies of importance. Even worse, with certain combinations of masses and spacing, resonance may occur. Resonance causes reduced insulation, which, in theory at least, can result in insulation below the value expected from one panel alone.

1.2. Literature Review

Noise transmission through aircraft fuselage wall is a major concern for the aircraft designers. Vibration absorbing engine mounts, single wall and double wall made of composite laminated panel, sandwich trim panels and sound proofing material has enabled reducing the noise level significantly. However, the sound insulation ability of "soundproof' cabins averages typically 30-50 dB for frequencies above 500 Hz, but only 0 – 19 dB for frequencies below 500 Hz. Various tonal and broadband noise components in this frequency range, e.g., buzz-saw noise, jet noise and the turbulent boundary layer, are perceived as very annoying. Reduction of low frequency noise requires a substantial increase in mass which for an aircraft is an untenable solution. To address this problem in the low frequency region, a detailed literature review is required in this frequency range.

Chladni [2] is often stated as the "father of acoustics" for his pioneering experimental works on acoustics involving plates having different geometries. However, Rayleigh [3] can be regarded as the pioneer who first addressed the connection between sound and vibration of strings, bars, membranes, plates and curved shells in the book titled 'The Theory of the Sound'. Research on structural-acoustic interaction problems started during World War II by various researchers like Lax (1944) [4], Fay (1948)[5], Finney (1948)[6] etc. These resulted in the founding steps in the theory of vibro-acoustic modelling and these days one can find quite a good number of books on acoustics by several authors (Morse & Ingard [7],Skudrzyk [8],Pierce [9], Kuttruff [10], Seto [11], Junge r& Feit [12], Fahy & Gardonio [13], Norton [14]). For the first time, the instrumentation techniques for experimental works were discussed by Beranek [15] in his book "Acoustic Measurements". At end of the last century an important work can be attributed to Crocker [16] who edited "Encyclopedia of Acoustics" where discussion are made on various topics of acoustics, viz., theories, application, noise reduction techniques, etc.

As the present work deals with energy transmission of structural panel connected to a semi cylindrical enclosure, literature has been studied for energy transmission through structural panel. The studies are presented in next three subsections, first one for Single wall, and next one for Double wall and at last for the Curved wall.

1.2.1 Literature Review for Energy Transmission through Single Wall

At low frequencies, one can calculate the sound transmission loss (STL) of a single panel with the mass law where the transmission loss of the panel depends only upon the frequency of the sound and the mass per unit area of the wall. Below the coincidence frequency the transverse bending wavelength of the panel in question is smaller than the wavelength of an acoustic wave in air at the same frequency. So, mass law is only valid below the coincidence frequency (f_c). Above this frequency, transmission of a reverberant field is dominated by resonance transmission associated with coincidence. Cremer [17] derived an empirical formula for frequency above the coincidence frequency incorporating the damping term. But this theory is limited up to twice the critical frequency. These two models combinedly is called as the Mass law-Cremer model. The agreement of this model

with experimental results is poor, especially at frequencies near coincidence. The disparity between the mass law-Cremer prediction and experiment at frequencies near coincidence, the so-called 'coincidence dip' - is well known, and others have tried to correct for this. Sharp[18] proposed a successful, empirical method to correct this effect. Since the mass law predicts the STL at frequencies greater than one-half the coincidence frequency so poorly, Sharp suggested using a linear interpolation scheme between the mass law STL at one-half of the *coincidence* frequency and the STL found with Cremer's expression at the coincidence frequency. This correction worked well reducing the disparity between predication and experiment in the range from $f_c/2$ to f_c.

There is still the problem of the under-prediction of the transmission loss at low frequencies (below $f_c/2$). Sewell [19] derived an expression based upon theoretical considerations of the forced transmission of sound through a partition incorporating various factors such as acoustic wavenumber, area of the plate, and shape factor correction for non-square plates. Sewell's expression, led to better agreement with experimental data at low frequencies than the mass law. This expression is for forced transmission and strictly speaking one should add the contribution from resonant transmission. However the resonant component is several dB lower than the forced component and will not affect the calculated transmission loss significantly.

To summarize the best agreement with experimental data was obtained with the Sewell-Sharp-Cremer or SSC model. This model suggests to follow Sewell expression for frequencies below $f_c/2$; from $f_c/2$ to f_c Sharp's linear interpolation scheme; above f_c from Cremer.

The inherent weakness of any STL prediction by SSC model is that the damping value affects the calculated STL above coincidence to a greater degree and this model gives a good estimate for flat surface with small dimension like windows or barriers or partition wall. The effect of boundary condition and material properties is not considered in this model. So, a different model is required to predict a damping value based on the above two conditions. But still the contribution of the stiffness term is ignored, which play very important role in real life problem. Another limitation of this model is that it is valid for normal incidences only.

London[20] introduced a theoretical model based on an impedance approach to estimate the sound transmission through homogeneous single walls considering the random incidence of sound waves. The attenuation was integrated over all angles of incidence to find the average transmission loss. Sound-transmission measurements were made and the results were found to be in satisfactory agreement with the theoretical treatment given by Cremer [17], which postulates that the wall impedance has a resistive component in addition to its mass reactance and a stiffness reactance resulting from the occurrence of flexural waves. He indicates three important physical properties of a homogeneous wall, namely, its mass, internal damping or dissipation, and its ability to propagate flexural waves, which determine its sound transmission loss. However, this method was sufficient only for nonresonant transmission.

Takahashi [21] developed an analytical model to predict the sound transmission through single plates with absorptive facings by taking into account the mass and impedance variation based on London Model. The results were found to be good at mid and high

frequencies. Later he improved the theory on several points regarding both the absorptive layer and acoustic coupling at the radiation boundary [22].

Beside the development of analytical models, some experimental works are also reported to validate that model. Beatty Jr. et al [23] had done small-scale measurements of transmission loss as a function of angle of incidence. The transmission loss, defined in terms of an average transmitted pressure, was found to be in rough agreement with Cremer's theory of the coincidence effect. The effects of damping and panel size were also discussed.

The modeling of the sound transmission characteristic gain advancement with the employment of Numerical techniques such as FE, BE and their combinations. Apart from these deterministic approaches, statistical energy analysis (SEA) based methods are used in the mid to high frequency vibro-acoustic analysis. Kuroki and Yasuoka [24] treated quantitatively the energy loss at the boundary of a single-leaf wall, as the internal loss factor is an important parameter in the case of calculating the transmission loss of a panel by using SEA.

1.2.2 Literature Review for Energy Transmission through Double Wall

The first well-known theoretical model to calculate the sound transmission loss (STL) of a double panel was probably introduced by London [25] in the year 1950 based on an impedance approach for obliquely sound wave incidence. He treated the double wall to be made up of two identical homogenous wall, and applied the impedance approach developed for single wall. A progressive-wave model was proposed and validated experimentally to estimate the transmission loss through a double-panel partition when subjected to a reverberant sound field. The attenuation was integrated over all angles of incidence to find the average transmission loss. It was shown in this research article that for reverberant sound field, customary normal incidence theory is inadequate to explain the behaviour of double wall partition. It was also numerically explained that for double wall partition, the modelling of individual single wall with a mass reactance behaviour is not sufficient to explain the transmission loss, effect of dissipation or resistance and flexural motion of the walls should also be included. Nevertheless, it is evident from the article that air coupling and filling of the gap with sound absorbing material shows an appreciable increase in the transmission loss. For double walls, if only air coupled, appreciable transmission loss over the single walls has been observed for very shallow airspaces. However, the method was sufficient only for nonresonant transmission and the most important issue that should be highlighted is that the frequency range of interest explored in this article ranges from 100 cps to 4000 cps which is about 630 Hz to 25 KHz. The model was then extended by Beranek [26], leading to the London-Beranek model for analysis of noise transmission through a double wall.

However, the model is restricted to the double-panel structure of infinite extent. For an infinite double-panel structure, panel stiffness plays an insignificant part in the energy transmission analysis which is not true for a finite structure due to the introduction of the panel resonance arising from the finite boundaries of the panel. Beranek [27] explained that the panel vibrates as a plate or a stretched membrane at low frequency and at higher

frequencies the panel may behave as a quasi-infinite sheet. It was been observed that the double wall panels at low frequencies near the mass-air-mass resonance are less efficient as the model for infinite panels reveal an out-of-phase motion of the two walls[28].

This analysis was later extended by Mulholland, Price and Parbrook [29] to random-incidence transmission, but was still restricted to non-resonant transmission. Theories for finite-size double panels have been formulated by Cummings and Mulholland [30] and by White and Powell [31]. The first one only gives reasonable results if an absorption coefficient of unity throughout the frequency range is chosen for the absorbing material at the edges of the cavity, which is unrealistic. The analysis given by White and Powell is restricted to purely resonant transmission and does not deal with the effect of sound-absorbing material placed in the cavity.

For calculating response of the structure due to acoustic excitation it is needed to sum up individually calculated response at each mode. But when the modal density is high (many closely spaced modes for complicated structure and mid to high frequency region) the deterministic approaches such as modal superposition technique takes huge computational time and cost. A solution of this problem is the statistical energy approach. The approach was used to study the transmission of random-incidence sound waves through a finite double-wall panel by Price and Crocker [32]. The study was performed for both resonant and nonresonant transmission by assuming double panel as a five coupled oscillator system, room-panel-cavity-room-panel-room. It was shown that the energy transmission depends upon the radiation resistance of the panels, the panel spacing, and the panel and cavity loss factors. Sound-absorbing material was placed around the edges of the cavity between the two panels. But the model was limited to mid to high frequency region.

There have been several efforts to reduce transmission through a double wall using active control. One of the earliest among them can be attributed to Sas et al [33]. They developed an analytical method based on modal coupling theory to explain the physical phenomenon underlying the behaviour of a coupled vibro-acoustic system. Subsequently a study was also carried out to explore the feasibility of improving the insertion loss of lightweight double panel partitions by using small loud speakers as active noise control sources inside the air gap between the two panels. It is shown that a considerable improvement of the insertion loss has been achieved around the lightly damped resonances of the system for the frequency range 60 to 220 Hz.

Several approaches have been put forward in the field of active noise control to increase the sound transmission loss of double-wall structures. However, for different circumstances, different approach is effective. Pan and Bao [34] carried an experimental study to explore the effectiveness of different control philosophies on the transmission characteristic of acoustic disturbance into an acoustic enclosure. The control philosophies implemented are (i) Room/Enclosure Control (ii) Cavity Control and (iii) Plate Vibration Control. It was shown that the transmission characteristics are governed by either modal suppression of the cavity mode or modal rearrangement. It was also pointed out by the authors that in certain cases, although there is a reduction in cavity pressure, structural vibration of the panel need not necessarily gets reduced. In a related work, Bao and Pan [35]

developed an analytical model to explain the transmission characteristic of sound through a double wall panel into a closed enclosure using the modal acoustic transfer impedance and mobility matrices. They used modal expansion method for fluid/acoustic and structural domain separately and obtained the coupling coefficients. They introduced three active control arrangements for double wall sound transmission similar to their experimental work. The analytical solution of the system response is used to explain the mechanisms of attenuation associated with these three control arrangements. While analyzing the physical mechanism of sound transmission it was shown (i) the secondary control source in the room/enclosure is effective only for the primary sound field dominated by a single room mode. (ii) Vibration control of the radiating structure can attenuate the sound pressure in the room. However, when several plate modes participate in the coupling with a dominating room mode, the control source rearranges itself in terms of magnitude and phase of the plate modes such that the superimposed sound radiation from the plate to the room is significantly reduced. (iii) The (0,0,0) cavity mode of the gap cavity between the two plates in the double wall partition is responsible for sound transmission in the low frequency and the suppression of this dominating mode in the cavity blocks the sound transmission path.

The sound transmission through the double wall panel reviewed so far did not consider any transfer path other than the acoustic gap between the panels. However, for all practical purposes the two panels are connected either with studs placed intermediately or mechanical connecters along the edges. These additional connections form the mechanical transfer path for the sound. One of the earliest literatures addressing the issue of the mechanical transfer path is due to Wang et al [36]. They considered two infinite panels connected by mechanical links or studs. Each stud is being modeled as a combination of linear and rotational spring. Plate bending equations assuming Kirchhoff's hypothesis are considered wherein the coupling between the structure and the acoustic domain is included in terms of pressure. During the same period Cheng et al [37] presented a model to estimate the transmissibility characteristic of a simply supported double wall connected with mechanical link and backed by an acoustic cavity. Following Green's Theorem a full coupling between the structural panels and the acoustic domain is modeled. Approximate method has been employed to estimate the structural and the acoustic mode shapes. A mode based vibro-acoustic coupling matrix is presented and they identified the behaviour of the acoustic and the mechanical transfer path separately. However the model is limited to estimation of the mode shapes and eigen frequencies as the variation of the boundary condition severely restricts the approximation procedure. In a subsequent work by Li and Cheng [38] a control mechanism is proposed to reduce sound transmission through a double wall partition. In their work they introduced both acoustic control and structural control concept. The acoustic control is achieved by placing a loud speaker in the air gap between the two panels. For structural control they introduced THUNDER actuators and reported the utility of both the acoustic and mechanical control in attenuating sound transmission.

1.2.3 Literature Review for Energy Transmission through Curved Wall

The investigation of sound transmission loss was started on flat plate or wall, later the behaviour of sound transmission through a curve surface is investigated. Probably Smith [39]

was first to investigate the sound transmission loss through a curved surface. He developed an analytical model based on impedance of the thin cylindrical elastic shell to an incident plane wave which is expressed as a sum of partial plane wave, was formulated as a function of axial wavelength and angular dependence of force. But the formulation was for infinitely long uniform cylindrical shell. A mathematical formula was evaluated in the literature for the ratio of power transmitted to the shell content to the power of the incident plane wave by evaluating the absorption cross section of the shell.

The work of Smith was extended by Koval [40] to include airflow external to the cylinder and internal shell pressurization to simulate airplane in flight condition. The change in transmission loss characteristics due to different flow condition and acoustic property was investigated. It is shown that, the cylinder transmission loss has dips at f_R (cylinder ring frequency) and f_c (critical frequency for a flat panel of the same material and thickness as shell). Below f_R, cylinder resonances affect transmission loss (TL). Between f_R and f_c, the cylinder TL follows a mass-law behaviour. The flow provides a modest increase in TL in the mass-law region, strongly interacts with the cylinder resonances below f_R, and tends to increase the frequency at which the f_c dip occurs. For normally incident waves, the TL is unaffected by flow. But it was assumed in the literature that the interior of the shell was totally absorbing. In the next work Koval [41] studied the effect of the cavity resonance on the sound transmission characteristics of the shell. It was concluded that cavity resonance in general leads to decrease of noise reduction. Modest internal absorption is shown to greatly reduce the effect of cavity resonances. The effects of external airflow, internal cabin pressurization, and different acoustical properties inside and outside the cylinder are also included in the study. Koval [42] also studied the sound transmission through stiffened shell. Ring frames and stringers were modelled as discrete structural elements. However, all of his studies were for infinite cylinders. The work of Koval on transmission loss (TL) by an orthotropic infinite cylindrical shell with one layer was extended by Blaise et al [43]. He introduces two independent angles (elevation and azimuth for incident plane wave), in order to calculate the diffuse field transmission coefficient (R_d).

Composite structures are used now-a-days in various engineering applications including aerospace, marine, and automotive applications because of the advantages offered by a high strength to weight ratio. An analytical model was developed by Daneshjou et al [44] to estimate sound transmission through an infinite laminated composite cylindrical shell. Comparison between composite and aluminium shell was also performed and it was concluded that though the composite shell behaves well in sound insulation below the ring frequency, it is not that much more effective than aluminium panel in mass controlled region and the structural damping becomes unimportant in the study of TL except at resonance frequencies.

A numerical approach based on a reacceptance method had been developed by Bilong et al [45] to evaluate the airborne sound insulation of aircraft panels with stringer and ring frame attachments. He showed for large curved aircraft panels the ring frames have little influence on the sound transmission loss in the frequency range of interest. However, the stringers may have considerable influence on the sound transmission loss. The stringer improves the sound transmission loss for a curved panel in the vicinity of the ring frequency,

but may result in a potential deterioration above this frequency. In addition, it was found that the sound transmission loss for the composite skin attached with composite stringers was lower than that of the metallic panel attached with metallic stringers.

An analytical study of sound transmission into semi cylindrical enclosures through discretely stiffened curved elastic panels is presented by Cheng et al [46]. The response characteristics of these panels are determined by using a modal analysis where the modes are obtained by the finite element-strip method. Numerical results include spectra of the interior sound pressure due to white noise, turbulent boundary layer and propeller noise inputs. This paper indicates, neglecting the effect of discrete stiffening can introduce significant errors and for lower frequencies, the noise transmission is also sensitive to the radius of the semi-cylindrical enclosure. It is also stated that, the acoustic absorption at the interior walls can also have a positive effect on noise attenuation by suppressing the acoustic resonances.

1.3. Objectives and Scope of Work

During the review process of the theory of the sound transmission mechanism through structural panels it is observed that the sound transmission mechanism through a single as well as a double wall semi-cylindrical panel with or without an enclosure is rare in the open literature. Whereas, the fuselage of aircraft can be considered similar to semi-cylindrical enclosure.

It is from this perspective the present work is attempted at developing a general methodology to suitably model the sound transmission mechanism through semi-cylindrical panel of a single wall. The scope of the work also includes the effect of various load conditions, such as point load, patch load, strip load at different positions or pressure load at different angles. Then, a study is carried out to understand the effect of damping of structural panel and acoustics and also the effect of increasing the thickness of the panel. Present work also includes study of the effect of different laminated composites. A separate model is developed for semi-cylindrical double wall structure of and the effect of thickness of air gap between two panels, the effect of different laminated composites on the sound transmission characteristics are studied.

1.4. Organisation of Thesis

The present thesis contains four chapters. Chapter 1, i.e., the present chapter contains the background and motivation of the present work. Single as well as double semi cylindrical panels are used in various structures, especially in aircraft fuselage. Sound transmission characteristics for these panels in the low frequency region are one of the main concerns for the application of these kinds of panels. The present work delves into the transmission characteristics of single and double semi cylindrical panels. A detailed review of the existing literature is presented in this chapter focusing the present work.

Chapter 2 deals with the mathematical formulation for sound energy transmission. The panels are discretised using isoparametric shell element and the acoustic domain is discretised using fluid element. Equation of motion for the panels and the wave equation for the acoustic portions are solved. Green's theorem is used for the coupling analysis. Free field sound radiation is formulated using free field Green's function and Kirchoff-Helmholtz free field radiation equation.

In Chapter 3, the finite element code in MATLAB platform and finite element model in ANSYS platform are validated with the results available in the literature. After the validation part, the model is prepared for semi-cylindrical single wall panel. Several case studies are performed for energy transmission characteristics, taking different loading condition such as point load, patch load, strip load applied at different positions and pressure load applied at different angles, different damping co-efficients, different wall thickness, orientation of lamina for laminated composites etc. A few case studies are shown for double wall panel for various air gap ratio, damping co-efficients and wall thickness.

Chapter 4 concludes the present work and some future scopes of work are highlighted. The list of references is presented at the end.

CHAPTER 2: MATHEMATICAL FORMULATION

2.1 Introduction:

Numerical modelling of coupled vibro-acoustics problem plays a major role in the design of many engineering structure, i.e. aircraft fuselage, sound barrier etc. Conducting experiment o the prototype of the desired structure is costly and time consuming. Whereas, a proper numerical modelling of the desired vibro-acoustics problem is very efficient. In this section numerical modelling of the present problem is worked out. This section is divided into two subsections. In the first subsection the coupled vibro-acoustic model for a single wall curved panel connected to a semi cylindrical enclosure is detailed. In this sub-section the mathematical basis of two-way coupled analysis is presented which is used to predict the interior noise level and to estimate the energy transmission. In the next sub-section developed model is extended for semi cylindrical double wall panels connected to the enclosure.

2.2 Coupled vibro-acoustic model for single wall panel connected to a semi cylindrical enclosure

In this section a coupled vibro-acoustic model is formulated for the single wall curved structure consisting of a semi cylindrical panel (defined with a subscript‘s’) connected to an acoustic enclosure as shown in Figure2.1. The acoustic enclosure is defined with a subscript ‘e’ and volume of the enclosure is V_e.

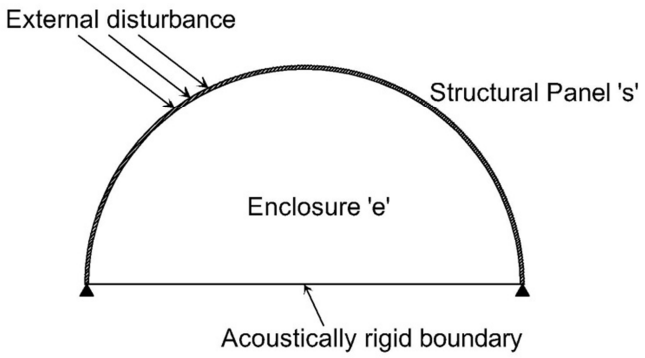

Figure 2.1: Coupled vibro-acoustic model for single wall panel connected to a semi cylindrical enclosure

In this model the panel excited by an external mechanical excitation and the vibrating panel influences the surrounding acoustic fluid.

The basic assumptions for the following formulation are:

i) The panels are made of either an isotropic or a laminated composite material.
ii) The panels are simply supported along their edges.
iii) The boundaries of the semi cylindrical enclosure are acoustically rigid except those boundaries which are attached to panel.

iv) External disturbance is harmonic in nature.
v) The fluid in the semi cylindrical enclosure is isotropic, homogeneous, inviscid and compressible.

In the mathematical formulation of the energy transmission, the equation of motion for the curved panel and the wave equation for the semi cylindrical enclosure are formulated. Then free vibration analysis is done for structural element as well as acoustic domain separately. Green's theorem is used to couple the structural components and the acoustical portion. Modal responses for different components of the system are calculated from the coupling analysis and then the overall responses are evaluated. The details of the model are elaborated in next few sub subsections.

2.2.1 Equation of motion for Structural Panel

The semi cylindrical curved panel in the present study is made of either an isotropic or a laminated composite material, as mentioned earlier. As the thickness of the structure is small compared to the other dimensions, first order shear deformation theory as proposed by Reissner-Mindlin is adopted in the present formulation with the modification for laminated composite plate given by Yang, Norris and Stavsky (YNS).The assumptions made are,

i) The thickness of the curved panel is small compared to other dimensions of the panel.
ii) Transverse stresses can be neglected.
iii) The normal to the mid-plane of the curved panel which is straight before deformation remains straight but not necessarily perpendicular to the mid-plane after deformation.

For numerical implementation of the mathematical modelling of the semi cylindrical curved panel, a finite element approach is used in the present thesis. The element chosen for the present analysis to discretize the structural panels are four node isoparametric shell finite elements with bilinear shape functions as shown in Figure 2.2. At each node of the element, five structural degrees of freedom are considered as shown in Figure 2.3.The mid-surface displacement field of the element in the local coordinate is expressed as,

$$\{d_e\} = \{u_{x0}, u_{y0}, u_{z0}, \theta_{x0}, \theta_{y0}\}^T$$

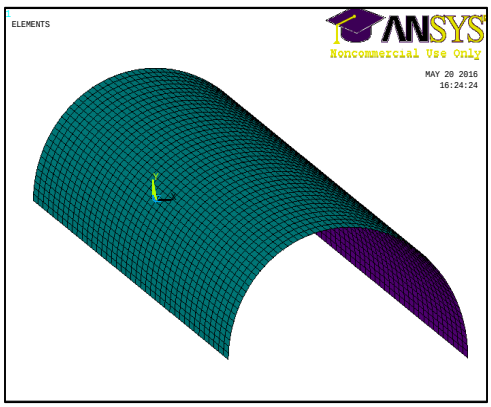

Figure 2.2: Finite element discretization model of semi cylindrical structural curved panel

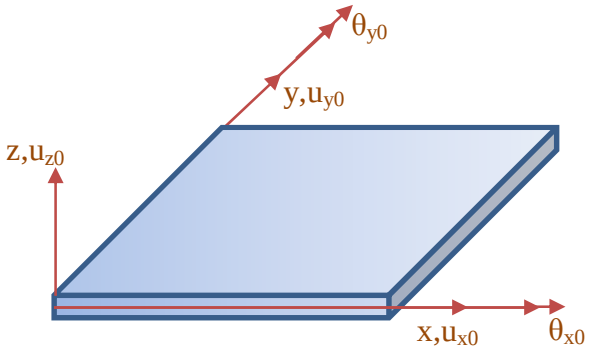

Figure 2.3: Mid-plane displacements in local coordinate of finite element

The displacement at any point (*x*,*y*,*z*) within the element can be represented in terms of the mid-plane displacement component as,

$$u_x = u_{x0} + z\theta_{y0} \tag{2.1a}$$

$$u_y = u_{y0} - z\theta_{x0} \tag{2.1b}$$

$$u_z = u_{z0} \tag{2.1c}$$

However the present analysis is performed in ANSYS platform and hence the finite element detailing and the development of strain-displacement relationship matrix and constitutive matrix are avoided to make the presentation concise. A brief write up on the ANSYS modelling and the description of element properties is presented later.

The governing dynamic equation for the structural panel can be obtained by applying Hamiltonian principle. The fundamental in the following formulation is the Hamiltonian principle which states that, "Of all the possible paths along which a dynamical system may move from one point to another within a specified time interval (consistent with any constraints), the actual path followed is that which minimizes the time integral of the total energy."

$$\int_{t_1}^{t_2}(\delta T - \delta U + \delta W_{nc})dt = 0 \tag{2.2}$$

where, T =kinetic energy

U=potential energy

W_{nc}=virtual work due to non-conservative forces

Variation of kinetic and potential energy and non-conservative work are expressed in terms of generalized independent displacements, velocities and forces assuming the total number of generalized independent displacements as 'r',

$$\delta T = \sum_{i=1}^{r}\left(\frac{\partial T}{\partial d_{ig}}\delta d_{ig} + \frac{\partial T}{\partial \dot{d}_{ig}}\delta \dot{d}_{ig}\right) \tag{2.3a}$$

$$\delta U = \sum_{i=1}^{r}\left(\frac{\partial V}{\partial d_{ig}}\delta d_{ig}\right) \tag{2.3b}$$

$$\delta W_{nc} = \sum_{i=1}^{r}\left(F_i \delta d_{ig}\right) \tag{2.3c}$$

d_{ig}=i^{th} generalized displacement of panel 'a' in global coordinate

$\dot{d}_{ig}$=i^{th} generalized velocity of panel 'a' in global coordinate

F_i=generalized force at i^{th} generalized coordinate

Eq. (2.2) and Eq. (2.3) are combined and expressed as,

$$\int_{t_1}^{t_2}\sum_{i=1}^{nd}\left[\left(\frac{\partial T}{\partial d_{ig}} - \frac{\partial U}{\partial d_{ig}} + F_i\right)\delta d_{ig} + \frac{\partial T}{\partial \dot{d}_{ig}}\delta \dot{d}_{ig}\right]dt = 0$$

$$\int_{t_1}^{t_2}\sum_{i=1}^{nd}\left(\frac{\partial T}{\partial d_{ig}} - \frac{\partial U}{\partial d_{ig}} + F_i - \frac{d}{dt}\left(\frac{\partial T}{\partial \dot{d}_{ig}}\right)\right)\delta d_{ig}dt = 0$$

Considering the arbitrariness of the virtual generalized displacement,

$$\frac{\partial T}{\partial d_{ig}} - \frac{\partial U}{\partial d_{ig}} + F_i - \frac{d}{dt}\left(\frac{\partial T}{\partial \dot{d}_{ig}}\right) = 0$$

$$\frac{d}{dt}\left(\frac{\partial T}{\partial \dot{d}_{ig}}\right) - \frac{\partial T}{\partial d_{ig}} + \frac{\partial U}{\partial d_{ig}} = F_i \tag{2.4}$$

Kinetic energy for an element is expressed as,

$$T_e = \frac{1}{2}\int_V \{\dot{d}_e\}^T[\rho]\{\dot{d}_e\}dV$$

$$= \tfrac{1}{2}\int_V \{\dot{d}_{en}\}^T[N_e]^T[\rho][N_e]\{\dot{d}_{en}\}\,dV \tag{2.5}$$

where, {ρ}=inertia matrix which can be computed from the equation of equilibrium of motion along x, y and z direction and finally written as,

$$[\rho] = \begin{bmatrix} I & 0 & 0 & 0 & P \\ 0 & I & 0 & -P & 0 \\ 0 & 0 & I & 0 & 0 \\ P & 0 & 0 & 0 & Q \\ 0 & P & 0 & -Q & 0 \end{bmatrix}; \quad I = \int_{-h/2}^{h/2}\rho_m dz, \quad P = \int_{-h/2}^{h/2} z\rho_m dz, \quad Q = \int_{-h/2}^{h/2} z^2\rho_m dz$$

ρ_m= density of material of Structural Panel

h= thickness of Structural Panel

Eq. (2.5) can be written as,

$$T_e = \frac{1}{2}\{\dot{d}_{en}\}^T[M_e]\{\dot{d}_{en}\}$$

where, $[M_e]$=elemental mass matrix=$\frac{1}{2}\int_V [N_e]^T[\rho][N_e]\,dV$

For the whole panel, the kinetic energy is defined as,

$$T = \frac{1}{2}\{\dot{d}_s\}^T[M_s]\{\dot{d}_s\} \quad (2.6)$$

where, $[M_s]$=mass matrix of structural panel

$\{\dot{d}_s\}$ = nodal velocity vector of structural panel

The Potential energy of an element is defined as,

$$U_e = \frac{1}{2}\{\epsilon_e\}^T\{\sigma_e\}$$

$$= \frac{1}{2}\{d_{en}\}^T[B_e]^T[D_e][B_e]\{d_{en}\}$$

$$= \frac{1}{2}\{d_{en}\}^T[K_e]\{d_{en}\}$$

where, $[K_e]$=elemental stiffness matrix=$[B_e]^T[D_e][B_e]$

For the whole system, the total potential energy is expressed as,

$$U = \frac{1}{2}\{d_s\}^T[K_s]\{d_s\} \quad (2.7)$$

where, $[K]$=stiffness matrix of structural panel

If the system is considered as a damped one, then the effect of damping can be taken into account implicitly by inserting the force term due to damping in the nonconservative force equation. So the total nonconservative force will be due to the combined effect of external load and damping as shown in,

$$F = [F_{es}] - [C_s]\{\dot{d}_s\} \quad (2.8)$$

where, $[C_s]$= damping matrix of structural panel

$[F_{es}]$ =total external force on structural panel

Using Eq. (2.6), Eq. (2.7) and Eq. (2.8) in Eq. (2.5), one can obtain equation of motion for each generalized coordinate. Combining all the equations for each generalized coordinate Eq. (2.9) is formulated.

$$[M_s]\{\ddot{d}_s\} + [C_s]\{\dot{d}_s\} + [K_s]\{d_s\} = [F_{es}] \quad (2.9)$$

It is already mentioned earlier that the FE modelling of the structural panel is developed in ANSYS platform. The curved structural panel is discretized using ‘SHELL 181’ element of ANSYS 11.0. The details of the selected element are presented in Table 2.1.

Table 2.1: Properties of 'Shell 181' element of ANSYS

Shape	Quadrilateral
No of nodes	Four
Degrees of freedom at each node	Six (3 translational and 3 rotational)
Input Parameters	Coordinates of nodes, Thickness of shell (Variable thickness at each node are allowed), **Material Properties** (This element is eligible for isotropic as well as orthotropic material) are EX, EY, EZ (Elastic modulus, plate element in x, y and z directions respectively) PRXY, PRYZ, PRXZ (Poisson's ratio, for plate element in x-y, y-z and x-z plane respectively) DENS(Mass density of plate element) GXY, GYZ, GXZ (Shear modulus, for plate element in x-y, y-z and x-z plane respectively) **Real Constant** is THETA (Angle of first surface direction, in degrees)

Eigenvalues and mode shapes are obtained from the modal analysis performed in ANSYS for the developed finite element model of curved panel. The figure of Shell 181 is given below,

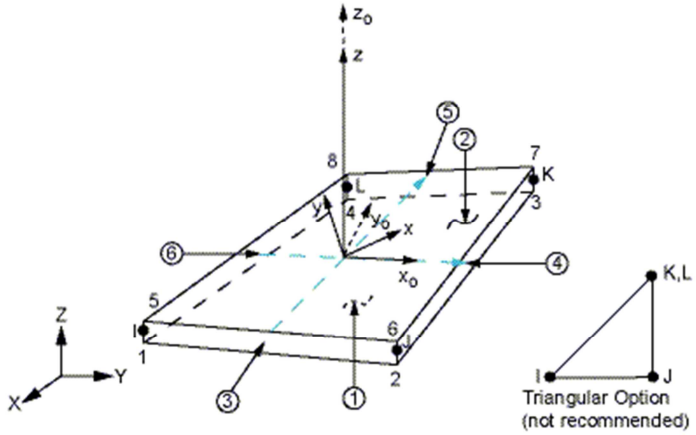

Figure 2.4: Shell 181 element

The forces acting on curved panel are external disturbances and force due to enclosure pressure,

$$[M_s]\{\ddot{d}_s\} + [C_s]\{\dot{d}_s\} + [K_s]\{d_s\} = \tilde{F}(t) - \int_{S_s} P_{es}(x, y, z, t)ds \quad (2.10)$$

where, $\tilde{F}(t)$ = external disturbance forceapplied at (x_i, y_i, z_i)on curved panel

$P_{es}(x, y, z, t)$ = acoustic pressure of the semi-cylindrical enclosure on curved panel

S_s = surface area of curved panel

Using the orthogonality property of mode shapes,

$$\{d_s\} = \sum_j \{\varphi_{s,j}\} q_{s,j}(t)$$

where, $\{\varphi_{s,j}\}$ = mode shape of curved panel at j^{th} mode

$q_{s,j}(t)$ = modal amplitude of displacement of curved panel at j^{th} mode

The equation of motion for curved panel at j^{th} mode is expressed as,

$$M_{s,j}\left[\ddot{q}_{s,j}(t) + 2\zeta_{s,j}\omega_{s,j}\dot{q}_{s,j}(t) + \omega_{s,j}^2 q_{s,j}(t)\right] = \tilde{F}\tilde{\varphi}_{s,j} - \int_{S_s} P_{es}\psi_{s,j}ds \quad (2.11)$$

where, $\tilde{\varphi}_{s,j}$=mode shape of the point where force acts

$M_{s,j}$ = generalized mass of curved panel at j^{th} mode

$\omega_{s,j}$ = natural frequency of curved panel at j^{th} mode

$\zeta_{s,j}$ = modal loss factor of curved panel at j^{th} mode

$\psi_{s,j}$ = mode shape of curved panel at j^{th} mode in the direction normal to the surface

2.2.2 Wave equation for the semi-cylindrical enclosure

The free vibration analysis of the semi-cylindrical enclosure has been performed in ANSYS. 'Fluid 30' element of ANSYS has been considered for discretization of the acoustic domain. The details of the selected element are presented in Table 2.2 with following assumptions:

i) The fluid is compressible (density changes due to pressure variations).

ii) Inviscid fluid (no dissipative effect due to viscosity).

iii) There is no mean flow of the fluid.

iv) The mean density and pressure are uniform throughout the fluid. Note that the acoustic pressure is the excess pressure from the mean pressure.

v) Analyses are limited to relatively small acoustic pressures so that the changes in density are small compared with the mean density.

Table 2.2: Properties of 'Fluid 30' element of ANSYS

Shape	Tetrahedron
No of nodes	Eight
Degrees of freedom at each node	1- Pressure + Additional 3-translations for fluid-structure interaction problem
Inputs	Nodal coordinates, Reference Pressure (PREF) = 20 x 10^{-6} N/m^2 The Speed of Sound (SONC) Density (DENS) Sound absorbing property (MU)

The governing equation for the acoustic pressure of the enclosed cavity is expressed as classical homogeneous wave equation,

$$\nabla^2 P_e - \frac{1}{c_e^2}\frac{\partial^2 P_e}{\partial t^2} = 0 \tag{2.12}$$

where, P_e = acoustic pressure of the semi-cylindrical enclosure

c_e =velocity of sound in the semi-cylindrical enclosure

Acoustic pressure is decomposed over the mode shapes of the semi-cylindrical enclosure,

$$\{P_e\} = \sum_m \{\varphi_{e,m}\} p_{e,m}(t) \tag{2.13}$$

Then the wave equation is rewritten as,

$$\nabla^2 \varphi_{e,m} = -\left(\frac{\omega_{e,m}}{c_e}\right)^2 \varphi_{e,m} \tag{2.14}$$

where, $\{\varphi_{e,m}\}$ = mode shape of the semi-cylindrical enclosure at m^{th} mode

$p_{e,m}(t)$ = modal pressure of the semi-cylindrical enclosure at m^{th} mode

$\omega_{e,m}$ = natural frequency of the semi-cylindrical enclosure at m^{th} mode

Generalized mass of the semi-cylindrical enclosure$M_{e,m}$is defined as,

$$\frac{1}{V_e}\int_{V_e} \{\varphi_{e,m}\}\{\varphi_{e,k}\} dv = \begin{cases} 0 & m \neq k \\ M_{e,m} & m = k \end{cases} \tag{2.15}$$

2.2.3 Coupling between panel and the enclosure

The pressure gradient of the acoustic domain at the coupling boundary is expressed in terms of inertia force due to the vibrating structural surface. The boundary condition is expressed as,

$$\frac{\partial P_e}{\partial \tilde{n}_e} = \begin{cases} \rho_e \ddot{w}_s & \text{on curve panel} \\ 0 & \text{on rigid wall} \end{cases} \quad (2.16)$$

where, ρ_e = equilibrium fluid density of enclosure

$\tilde{n}_e$=normal direction directed outwards from enclosure boundary

w_s= normal component of the structural displacements of curved panel

Green's theorem is used for two scalar functions P_e and $\varphi_e$smooth and non-singular in domain V_e enclosed by surfaceS_s and expressed as,

$$\int_{V_e} (P_e \nabla^2 \varphi_e - \varphi_e \nabla^2 P_e)\, dv = \int_{S_s} (P_e \frac{\partial \varphi_e}{\partial n} - \varphi_e \frac{\partial P_e}{\partial n}) ds \quad (2.17)$$

Using Eq. (2.12) to Eq. (2.14), for m^{th} mode of the air gap, Eq. (2.17) is written as,

$$\int_{V_e} \left[-\varphi_{e,m} p_{e,m}(t) \left(\frac{\omega_{e,m}}{c_e}\right)^2 \varphi_{e,m} - \varphi_{e,m} \frac{1}{c_e^2} \varphi_{e,m} \ddot{p}_{e,m}(t) \right] dv = -\int_{S_s} \varphi_{e,m} \rho_e \ddot{w}_s \, ds$$

Using Eq. (2.14),

$$\frac{M_{e,m} V_e}{c_e^2} \left[\omega_{e,m}^2 p_{e,m}(t) + \ddot{p}_{e,m}(t) \right] = \rho_e \sum_j \int_{S_s} \varphi_{e,m} \psi_{s,j} ds \, \ddot{q}_{s,j}(t) \quad (2.18)$$

The modal coupling coefficient may be expressed as follows,

$$L_{m,j}^{se} = \frac{1}{S_s} \int_{S_s} \varphi_{e,m} \psi_{s,j} ds$$

$L_{m,j}^{se}$ =modal coupling coefficient between the acoustical mode 'm' of the semi-cylindrical and the structural mode j of panel 's'

Introducing modal loss factor term, Eq. (2.18) is expressed as,

$$\ddot{p}_{e,m}(t) + 2\zeta_{e,m} \omega_{e,m} \dot{p}_{e,m}(t) + \omega_{e,m}^2 p_{e,m}(t) = \frac{\rho_e c_e^2}{M_{e,m} V_e} \left[S_s \sum_j L_{m,j}^{se} \ddot{q}_{s,j}(t) \right] \quad (2.19)$$

where,$\zeta_{e,m}$= modal loss factor of the semi-cylindrical enclosure at m^{th} mode

2.2.4 Response Calculation

The applied excitation is assumed to be harmonic in nature as shown in Eq. 2.20a. Then the modal coordinates of the panel and the modal pressure of the enclosure are also be expressed in the harmonic form as shown in Eq. 2.20b to Eq. 2.20c.

$$\tilde{F}(t) = F_0 e^{i\omega t} \tag{2.20a}$$

$$q_{s,j}(t) = \tilde{q}_{s,j} e^{i\omega t} \tag{2.20b}$$

$$p_{e,n}(t) = \tilde{p}_{e,n} e^{i\omega t} \tag{2.20c}$$

where, ω = excitation frequency

F_0 = amplitude of harmonic forcing

$\tilde{q}_{s,j}$ = amplitude of modal coordinates of curved panel at mode j

$\tilde{p}_{e,n}$ = amplitude of modal pressure of the enclosure at mode n

i = complex quantity = $\sqrt{-1}$

Applying harmonic condition in Eq. (2.10) and can be written as,

$$M_{s,j}\left[\omega_{s,j}^2 + 2i\zeta_{s,j}\omega_{s,j}\omega - \omega^2\right]\tilde{q}_{s,j} = \left\{F_0\varphi_{s,j}(x_i, y_i, z_i) - \sum_m \left(\int_{S_s} \varphi_{e,m}\psi_{s,j} ds\right)\tilde{p}_{e,m}\right\}$$

$$\Rightarrow \left[M_{s,j}\left(\omega_{s,j}^2 + 2i\zeta_{s,j}\omega_{s,j}\omega - \omega^2\right)\right]\tilde{q}_{s,j} + S_s\sum_m L_{m,j}^{se}\tilde{p}_{e,m} = \left\{F_0\varphi_{s,j}(x_i, y_i, z_i)\right\} \tag{2.21}$$

Applying harmonic condition in Eq. (2.19) and can be written as,

$$\left[\omega_{e,m}^2 + 2i\zeta_{e,m}\omega_{e,m}\omega - \omega^2\right]\tilde{p}_{e,m} = \frac{\rho_e c_e^2(-\omega^2)}{V_e}\left[\frac{S_s}{M_{e,m}}\sum_j L_{m,j}^{se}\tilde{q}_{s,j}\right]$$

$$\frac{\rho_e c_e^2 S_s \omega^2}{V_e}\frac{1}{M_{e,m}}\sum_j L_{m,j}^{se}\tilde{q}_{s,j} + \left[\omega_{e,m}^2 + 2i\zeta_{e,m}\omega_{e,m}\omega - \omega^2\right]\tilde{p}_{e,m} = 0 \tag{2.22}$$

Eq. (2.21) to Eq. (2.22) are assembled after taking the effects of the entire structural and acoustics modes and is described in matrix form,

$$\begin{bmatrix} H_{11} & H_{12} \\ H_{21} & H_{22} \end{bmatrix}\begin{Bmatrix} \tilde{q}_s \\ \tilde{q}_e \end{Bmatrix} = \begin{Bmatrix} F_s \\ 0 \end{Bmatrix} \tag{2.23}$$

F_s= generalized force applied to the curved panel

$\tilde{q}_s$ = modal responses of the curved panel = $\{\tilde{q}_{s,1}, \tilde{q}_{s,2}, \dots, \tilde{q}_{s,nms}\}^T$

nms = total no of modes taken into account for the curved panel

$\tilde{p}_e$ = modal responses of the enclosure = $\{\tilde{p}_{e,1}, \tilde{p}_{e,2}, \dots, \tilde{p}_{e,nme}\}^T$

nme = total no of modes taken into account for the enclosure

H_{11} = Modal dynamic stiffness of curved panel

$$= \begin{bmatrix} \ddots & 0 & 0 \\ 0 & M_{s,j}\left[\omega_{s,j}^2 + 2i\zeta_{s,j}\omega_{s,j}\omega - \omega^2\right] & 0 \\ 0 & 0 & \ddots \end{bmatrix}_{nms \times nms}$$

H_{12} = Coupling coefficients representing the effect of acoustic pressure of the enclosure on the structural response on curved panel

$$= S_s \begin{bmatrix} L_{1,1}^{se} & \cdots & L_{nme,1}^{se} \\ \cdots & \cdots & \cdots \\ L_{1,nms}^{se} & \cdots & L_{nme,nms}^{se} \end{bmatrix}_{nms \times nme}$$

H_{21} = Coupling coefficients representing the effect of the structural vibration of panel 'a' on the cavity pressure

$$= \frac{\rho_e c_e^2 S_s \omega^2}{V_e} \begin{bmatrix} \frac{1}{M_{e,1}}\left[L_{1,1}^{se}, \cdots, L_{1,nms}^{se}\right] \\ \vdots \\ \frac{1}{M_{e,nme}}\left[L_{nme,1}^{se}, \cdots, L_{nme,nms}^{se}\right] \end{bmatrix}_{nme \times nms}$$

H_{22} = Modal dynamic stiffness of the enclosure

$$= \begin{bmatrix} \ddots & & \\ & \left[\omega_{e,n}^2 + 2i\zeta_{e,n}\omega_{e,n}\omega - \omega^2\right] & \\ & & \ddots \end{bmatrix}_{nme \times nme}$$

Modal responses are expressed as,

$$\begin{Bmatrix} \tilde{q}_s \\ \tilde{p}_e \end{Bmatrix} = \begin{bmatrix} H_{11} & H_{12} \\ H_{21} & H_{22} \end{bmatrix}^{-1} \begin{Bmatrix} F_S \\ 0 \end{Bmatrix} \tag{2.24}$$

2.2.5 Energy transmission parameters

Energy transmission from curved panel to the enclosure is parameterized using Average quadratic velocity$\langle \mathbf{V}^2 \rangle$ of curved panel. The parameter characterizes velocity of every element and reflects the average value of square of velocities as shown in Eq. (2.25).Averaged quadratic velocity$\langle \mathbf{V^2} \rangle$is expressed in dB referenced to 2.5 X 10^{-15} m^2s^{-2}.

$$\text{Averaged quadratic velocity } \langle \mathbf{V^2} \rangle \text{ of curved panel} = \frac{\omega^2}{2S_s}\int_{S_s} w_s w_s^* ds \tag{2.25}$$

where, w_s^* = conjugate of displacement of panel 's'

Acoustic energy transmitted to enclosure, is quantified using averaged sound pressure level of the enclosure $L_{p,e}$.Averaged sound pressure level is a measure of averaged quadratic pressure with respect to square of reference sound pressure. The averaged sound pressure level of the enclosure is formalized in Eq. (2.26) to Eq. (2.27).

$$L_{p,e} = 10\log\left(\langle P_e^2\rangle / P_{ref}^2\right) \tag{2.26}$$

$$\langle P_e^2\rangle = \frac{1}{2V_e}\int_{V_e} P_e P_e^* dv \tag{2.27}$$

where, Reference pressure,P_{ref}= 20 μPa.

P_e^* = Complex conjugate of the acoustic pressure in the enclosure.

2.3 Coupled vibro-acoustic model for double wall panel connected to a semi cylindrical enclosure

Now the coupled vibro-acoustic model is extended for the double wall curved structure consisting of two concentric semi cylindrical shell panels separated by an air-gap and connected to an acoustic enclosure as shown in Figure 2.5. The gap cavity is defined with a subscript 'g' and volume of the gap cavity is V_g. The acoustic enclosure is defined with a subscript 'e' and volume of the enclosure is V_e. In present model it is assumed that, the primary source panel (panel 'a') excited by an external disturbance and the secondary panel (panel 'b') radiates sound into the enclosed field. The details of the model are elaborated in next few sub subsections.

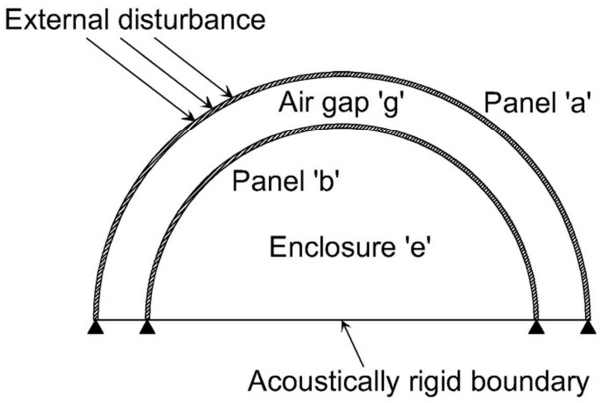

Figure 2.5: Coupled vibro-acoustic model for double wall panel connected to a semi cylindrical enclosure

2.3.1 Equation of motion for panel 'a'

Equation of motion for panel 'a' may be formulated in the similar fashion as derived for curved panel in the single wall model. The finite element formulation for the panel is also performed in ANSYS using 'Shell 181' element. Force on panel 'a' will be external disturbances and force due to gap cavity pressure. Thus, governing equation for vibration of panel 'a' may be expressed as,

$$[M_a]\{\ddot{d}_a\} + [C_a]\{\dot{d}_a\} + [K_a]\{d_a\} = \tilde{F}(t) - \int_{S_a} P_{ga}(x, y, z, t)ds \qquad (2.28)$$

where, $\tilde{F}(t)$ = external disturbance force applied at (x_i, y_i, z_i)on panel 'a'

$P_{ga}(x, y, z, t)$ = acoustic pressure of the air gap on panel 'a'

S_a = surface area of panel 'a'

Using the orthogonality property of mode shapes,

$$\{d_a\} = \sum_j \{\varphi_{a,j}\} q_{a,j}(t)$$

where, $\{\varphi_{a,j}\}$ = mode shape of panel 'a' at j^{th} mode

$q_{a,j}(t)$ = modal amplitude of displacement of panel 'a' at j^{th} mode

The equation of motion for panel 'a' at j^{th} mode is expressed as,

$$M_{a,j}\left[\ddot{q}_{a,j}(t) + 2\zeta_{a,j}\omega_{a,j}\dot{q}_{a,j}(t) + \omega_{a,j}^2 q_{a,j}(t)\right] = \tilde{F}\tilde{\varphi}_{a,j} - \int_{S_a} P_{ga}\psi_{a,j}ds \qquad (2.29)$$

where, $\tilde{\varphi}_{a,j}$=mode shape of the point where force acts

$M_{a,j}$ = generalized mass of panel 'a' at j^{th} mode

$\omega_{a,j}$ = natural frequency of panel 'a' at j^{th} mode

$\zeta_{a,j}$ = modal loss factor of panel 'a' at j^{th} mode

$\psi_{a,j}$ = mode shape of panel 'a' at j^{th} mode in the direction normal to the surface

2.3.2 Equation of motion for Panel 'b'

Equation of motion for panel 'b' may be formulated in the similar fashion as derived for panel 'a' in the previous subsection. The finite element formulation for the panel is also performed in ANSYS using 'Shell 181' element. Force on panel 'b' will be due to gap cavity pressure and pressure of the enclosure. Thus governing equation for vibration of panel 'b' may be expressed as,

$$[M_b]\{\ddot{d}_b\} + [C_b]\{\dot{d}_b\} + [K_b]\{d_b\} = \int_{S_b} P_{gb}(x,y,z,t)ds - \int_{S_b} P_{eb}(x,y,z,t)ds \qquad (2.30)$$

where. $\{d_b\}$ = displacement of panel 'b'

$[M_b], [C_b], [K_b]$ = mass, damping and stiffness matrix of panel 'b' respectively

$P_{gb}(x,y,z,t)$ = acoustic pressure of the air gap cavity on panel 'b'

$P_{eb}(x,y,z,t)$ = acoustic pressure of the enclosure on panel 'b'

S_b = surface area of panel 'b'

Using the orthogonal property of mode shapes,

$$\{d_b\} = \sum_k \{\varphi_{b,k}\} q_{b,k}(t)$$

where, $\{\varphi_{b,k}\}$ = mode shape of panel 'b' at k^{th} mode

$q_{b,k}(t)$ = modal coordinate of panel 'b' at k^{th} mode

The equation of motion for panel 'b' at k^{th} mode is expressed as,

$$M_{b,k}\left[\ddot{q}_{b,k}(t) + 2\zeta_{b,k}\omega_{b,k}\dot{q}_{b,k}(t) + \omega_{b,k}^2 q_{b,k}(t)\right] = \int_{S_b} P_{gb}\psi_{b,k}ds - \int_{S_b} P_{eb}\psi_{b,k}ds \qquad (2.31)$$

where, $M_{b,k}$ = generalized mass of panel 'b' at k^{th} mode

$\omega_{b,k}$ = natural frequency of panel 'b' at k^{th} mode

$\zeta_{b,k}$ = modal loss factor of panel 'b' at k^{th} mode

$\psi_{b,k}$ = mode shape of panel 'b' at k^{th} mode in the direction normal to the surface

2.3.3 Wave equation for the gap cavity

The FEM model of gap cavity has been done in ANSYS using the same element as stated for single wall model for enclosure. The governing equation for the acoustic pressure of the gap cavity is expressed as classical homogeneous wave equation,

$$\nabla^2 P_g - \frac{1}{c_g^2}\frac{\partial^2 P_g}{\partial t^2} = 0 \tag{2.32}$$

where, P_g = acoustic pressure of the air gap cavity

c_g =velocity of sound in the air gap cavity

Acoustic pressure is decomposed over the mode shapes of the gap cavity.

$$\{P_g\} = \sum_m \{\varphi_{g,m}\} p_{g,m}(t) \tag{2.33}$$

Then the wave equation is rewritten as,

$$\nabla^2 \varphi_{g,m} = -\left(\frac{\omega_{g,m}}{c_g}\right)^2 \varphi_{g,m} \tag{2.34}$$

where, $\{\varphi_{g,m}\}$ = mode shape of the air gap cavity at m^{th} mode

$p_{g,m}(t)$ = modal pressure of the air gap cavity at m^{th} mode

$\omega_{g,m}$ = natural frequency of the air gap cavity at m^{th} mode

Generalized mass of the gap cavity $M_{g,m}$is defined as,

$$\frac{1}{V_g}\int_{V_g}\{\varphi_{g,m}\}\{\varphi_{g,k}\}dv = \begin{cases} 0 & m \neq k \\ M_{g,m} & m = k \end{cases} \tag{2.35}$$

The development of the wave equation for enclosure is same as discussed for single wall model.

2.3.4 Wave equation for the enclosure

The FEM model of the enclosure for double wall has been done in ANSYS using the same element and in a similar fashion as stated for single wall model for enclosure.

The wave equation is for enclosure is,

$$\nabla^2 \varphi_{e,m} = -\left(\frac{\omega_{e,m}}{c_e}\right)^2 \varphi_{e,m} \tag{2.36}$$

where, $\{\varphi_{e,m}\}$ = mode shape of the semi-cylindrical enclosure at m^{th} mode

$p_{e,m}(t)$ = modal pressure of the semi-cylindrical enclosure at m^{th} mode

$\omega_{e,m}$ = natural frequency of the semi-cylindrical enclosure at m^{th} mode

Generalized mass of the semi-cylindrical enclosure$M_{e,m}$is defined as,

$$\frac{1}{V_e}\int_{V_e}\{\varphi_{e,m}\}\{\varphi_{e,k}\}dv = \begin{cases} 0 & m \neq k \\ M_{e,m} & m = k \end{cases} \quad (2.37)$$

2.3.5 Coupling between panels, gap cavity and the enclosure

The pressure gradient of the acoustic domain at the coupling boundary is expressed in terms of inertia force due to the vibrating structural surface. The boundary condition is expressed as,

$$\frac{\partial P_g}{\partial \tilde{n}_g} = \begin{cases} \rho_g \ddot{w}_a \text{ on panel 'a'} \\ -\rho_g \ddot{w}_b \text{ on panel 'b'} \\ 0 \text{ on rigid wall} \end{cases} \quad (2.38)$$

where, ρ_g = equilibrium fluid density of the gap cavity

$\tilde{n}_g$= normal direction directed outwards from gap cavity boundary

w_a= normal component of the structural displacements of panel ‘a’

w_b= normal component of the structural displacements of panel ‘b’

For the enclosure the boundary constraint is expressed as,

$$\frac{\partial P_e}{\partial \tilde{n}_e} = \begin{cases} \rho_e \ddot{w}_b \text{ on panel 'b'} \\ 0 \text{ on rigid wall} \end{cases} \quad (2.39)$$

where, ρ_e = equilibrium fluid density of enclosure

$\tilde{n}_e$= normal direction directed outwards from enclosure boundary

Green’s theorem is used for two scalar functions P_g and $\varphi_g$smooth and non-singular in domain V_g enclosed by surfaceS_a and S_b and expressed as,

$$\int_{V_g}\left(P_g\nabla^2\varphi_g - \varphi_g\nabla^2 P_g\right) dv = \int_{S_a+S_b}\left(P_g\frac{\partial\varphi_g}{\partial n} - \varphi_g\frac{\partial P_g}{\partial n}\right)ds \quad (2.40)$$

Using Eq. (2.32) to Eq. (2.34), for m^{th} mode of the air gap, Eq. (2.40) is written as,

$$\int_{V_g}\left[-\varphi_{g,m}p_{g,m}(t)\left(\frac{\omega_{g,m}}{c_g}\right)^2\varphi_{g,m}-\varphi_{g,m}\frac{1}{c_g^2}\varphi_{g,m}\ddot{p}_{g,m}(t)\right]dv =$$

$$-\int_{S_a}\varphi_{g,m}\rho_g\ddot{w}_a\,ds+\int_{S_b}\varphi_{g,m}\rho_g\ddot{w}_b\,ds$$

Using Eq. (2.35),

$$\frac{M_{g,m}V_g}{c_g^2}\left[\omega_{g,m}^2p_{g,m}(t)+\ddot{p}_{g,m}(t)\right]=\rho_g\left[\sum_j\int_{S_a}\varphi_{g,m}\psi_{a,j}ds\,\ddot{q}_{a,j}(t)-\sum_k\int_{S_b}\varphi_{g,m}\,\psi_{b,k}ds\,\ddot{q}_{b,k}(t)\right] \tag{2.41}$$

The modal coupling coefficient may be expressed as follows,

$$L_{m,j}^{ag}=\frac{1}{S_a}\int_{S_a}\varphi_{g,m}\psi_{a,j}ds \quad \text{and} \quad L_{m,k}^{bg}=\frac{1}{S_b}\int_{S_b}\varphi_{g,m}\psi_{b,k}ds$$

$L_{m,j}^{ag}$ =modal coupling coefficient between the acoustical mode m of the gap cavity and the structural mode j of panel ‘a’

$L_{m,k}^{bg}$= modal coupling coefficient between the acoustical mode m of the gap cavity and the structural mode k of panel ‘b’

Introducing modal loss factor term, Eq. (2.41) is expressed as,

$$\ddot{p}_{g,m}(t)+2\zeta_{g,m}\omega_{g,m}\dot{p}_{g,m}(t)+\omega_{g,m}^2p_{g,m}(t)=\frac{\rho_gc_g^2}{M_{g,m}V_g}\left[S_a\sum_j L_{m,j}^{ag}\ddot{q}_{a,j}(t)-S_b\sum_k L_{m,k}^{bg}\ddot{q}_{b,k}(t)\right] \tag{2.42}$$

where,$\zeta_{g,m}$= modal loss factor of the air gap at m^{th} mode

Similarly, coupling between enclosure and panel ‘b’ is expressed as,

$$\ddot{p}_{e,n}(t)+2\zeta_{e,n}\omega_{e,n}\dot{p}_{e,n}(t)+\omega_{e,n}^2p_{e,n}(t)=\frac{\rho_ec_e^2}{m_{e,n}V_e}\left[S_b\sum_k L_{n,k}^{be}\ddot{q}_{b,k}(t)\right] \tag{2.43}$$

where, $\zeta_{e,n}$= modal loss factor of the enclosure at mode n

$L_{n,k}^{be}$= modal coupling coefficient between the acoustical mode n of the enclosure and the structural mode k of panel ‘b’

$$L_{n,k}^{be}=\frac{1}{S_b}\int_{S_b}\varphi_{e,n}\psi_{b,k}ds \tag{2.44}$$

2.3.6 Response Calculation

The applied excitation is assumed to be harmonic in nature as shown in Eq. 2.45a. Then the modal coordinates of the panels and the modal pressures of the gap cavity and the enclosure are also be expressed in the harmonic form as shown in Eq. 2.45b to Eq. 2.45e.

$$\tilde{F}(t) = F_0 e^{i\omega t} \quad (2.45a)$$

$$q_{a,j}(t) = \tilde{q}_{a,j} e^{i\omega t} \quad (2.45b)$$

$$q_{b,k}(t) = \tilde{q}_{b,k} e^{i\omega t} \quad (2.45c)$$

$$p_{g,m}(t) = \tilde{p}_{g,m} e^{i\omega t} \quad (2.45d)$$

$$p_{e,n}(t) = \tilde{p}_{e,n} e^{i\omega t} \quad (2.45e)$$

where, ω = excitation frequency

F_0 = amplitude of harmonic forcing

$\tilde{q}_{a,j}$ = amplitude of modal coordinates of panel 'a' at mode j

$\tilde{q}_{b,k}$ = amplitude of modal coordinates of panel 'b' at mode k

$\tilde{p}_{g,m}$ = amplitude of modal pressure of the gap cavity at mode m

$\tilde{p}_{e,n}$ = amplitude of modal pressure of the enclosure at mode n

i = complex quantity = $\sqrt{-1}$

Applying harmonic condition Eq. (2.29) can be written as,

$$M_{a,j}\left[\omega_{a,j}^2 + 2i\zeta_{a,j}\omega_{a,j}\omega - \omega^2\right]\tilde{q}_{a,j} = \left\{F_0\varphi_{a,j}(x_e, y_e, z_e) - \sum_m \left(\int_{S_a} \varphi_{g,m}\psi_{a,j} ds\right)\tilde{p}_{g,m}\right\}$$

$$\Rightarrow \left[M_{a,j}\left(\omega_{a,j}^2 + 2i\zeta_{a,j}\omega_{a,j}\omega - \omega^2\right)\right]\tilde{q}_{a,j} + S_a \sum_m L_{m,j}^{ag}\tilde{p}_{g,m} = \left\{F_0\varphi_{a,j}(x_e, y_e, z_e)\right\} \quad (2.46)$$

Applying harmonic condition Eq. (2.31) can be written as,

$$M_{b,k}\left[\omega_{b,k}^2 + 2i\zeta_{b,k}\omega_{b,k}\omega - \omega^2\right]\tilde{q}_{b,k} = \sum_m \left(\int_{S_b} \varphi_{g,m}\psi_{b,k} ds\right)\tilde{p}_{g,m} - \sum_n \left(\int_{S_b} \varphi_{e,n}\psi_{b,k} ds\right)\tilde{p}_{e,n}$$

$$\Rightarrow \left[M_{b,k}\left(\omega_{b,k}^2 + 2i\zeta_{b,k}\omega_{b,k}\omega - \omega^2\right)\right]\tilde{q}_{b,k} - S_b \sum_m L_{m,k}^{bg}\tilde{p}_{g,m} + S_b \sum_n L_{n,k}^{be}\tilde{p}_{e,n} = 0 \quad (2.47)$$

Applying harmonic condition Eq. (2.42) is written as,

$$\left[\omega_{g,m}^2 + 2i\zeta_{g,m}\omega_{g,m}\omega - \omega^2\right]\tilde{p}_{g,m} = \frac{\rho_g c_g^2(-\omega^2)}{V_g}\left[\frac{S_a}{M_{g,m}}\sum_j L_{m,j}^{ag}\tilde{q}_{a,j} - \frac{S_b}{M_{g,m}}\sum_k L_{m,k}^{bg}\tilde{q}_{b,k}\right]$$

$$\frac{\rho_g c_g^2 S_a\omega^2}{V_g}\frac{1}{M_{g,m}}\sum_j L_{m,j}^{ag}\tilde{q}_{a,j} - \frac{\rho_g c_g^2 S_b\omega^2}{V_g}\frac{1}{M_{g,m}}\sum_k L_{m,k}^{bg}\tilde{q}_{b,k} + \left[\omega_{g,m}^2 + 2i\zeta_{g,m}\omega_{g,m}\omega - \omega^2\right]\tilde{p}_{g,m} = 0 \quad (2.48)$$

Applying harmonic condition Eq. (2.43) may be written as,

$$\left[\omega_{e,n}^2 + 2i\zeta_{e,n}\omega_{e,n}\omega - \omega^2\right]\tilde{p}_{e,n} = \frac{\rho_e c_e^2(-\omega^2)}{V_e}\left[\frac{S_b}{m_{e,l}}\sum_k L_{n,k}^{be}\tilde{q}_{b,k}\right]$$

$$\Rightarrow \frac{\rho_e c_e^2 S_b \omega^2}{V_e}\frac{1}{m_{e,l}}\sum_k L_{n,k}^{be}\,\tilde{q}_{b,k} + \left[\omega_{e,n}^2 + 2i\zeta_{e,n}\omega_{e,n}\omega - \omega^2\right]\tilde{p}_{e,n} = 0 \qquad (2.49)$$

Eq. (2.46) to Eq. (2.49) are assembled after taking the effects of the entire structural and acoustics modes and is described in matrix form,

$$\begin{bmatrix} H_{11} & 0 & H_{13} & 0 \\ 0 & H_{22} & H_{23} & H_{24} \\ H_{31} & H_{32} & H_{33} & 0 \\ 0 & H_{42} & 0 & H_{44} \end{bmatrix}\begin{Bmatrix} \tilde{q}_a \\ \tilde{q}_b \\ \tilde{p}_g \\ \tilde{p}_e \end{Bmatrix} = \begin{Bmatrix} F_a \\ 0 \\ 0 \\ 0 \end{Bmatrix} \qquad (2.50)$$

F_a= generalized force applied to the panel 'a'

$\tilde{q}_a$ = modal responses of the panel 'a' = $\{\tilde{q}_{a,1}, \tilde{q}_{a,2}, \dots, \tilde{q}_{a,nma}\}^T$

nma = total no of modes taken into account for the panel 'a'

$\tilde{q}_b$ = modal responses of the panel 'b' = $\{\tilde{q}_{b,1}, \tilde{q}_{b,2}, \dots, \tilde{q}_{b,nmb}\}^T$

nmb = total no of modes taken into account for the panel 'b'

$\tilde{p}_g$ = modal responses of the gap cavity = $\{\tilde{p}_{g,1}, \tilde{p}_{g,2}, \dots, \tilde{p}_{g,nmg}\}^T$

nmg = total no of modes taken into account for the gap cavity

$\tilde{p}_e$ = modal responses of the gap cavity = $\{\tilde{p}_{e,1}, \tilde{p}_{e,2}, \dots, \tilde{p}_{e,nme}\}^T$

nme = total no of modes taken into account for the enclosure

H_{11} = Modal dynamic stiffness of curved panel 'a'

$$= \begin{bmatrix} \ddots & & \\ & M_{a,j}\left[\omega_{a,j}^2 + 2i\zeta_{a,j}\omega_{a,j}\omega - \omega^2\right] & \\ & & \ddots \end{bmatrix}_{nma \times nma}$$

H_{13} = Coupling coefficients representing the effect of acoustic pressure of the gap cavity on the structural response on panel 'a'

$$= S_a \begin{bmatrix} L_{1,1}^{ag} & \cdots & L_{nmg,1}^{ag} \\ \cdots & \cdots & \cdots \\ L_{1,nma}^{ag} & \cdots & L_{nmg,nma}^{ag} \end{bmatrix}_{nma \times nmg}$$

H_{22} = Modal dynamic stiffness of curved panel 'b'

$$= \begin{bmatrix} \ddots & & \\ & m_{b,k}\left[\omega_{b,k}^2 + 2i\zeta_{b,k}\omega_{b,k}\omega - \omega^2\right] & \\ & & \ddots \end{bmatrix}_{nmb \times nmb}$$

H_{23} = Coupling coefficients representing the effect of acoustic pressure of the gap cavity on the structural response on panel ‘b’

$$= -S_b \begin{bmatrix} L^{bg}_{1,1} & \cdots & L^{bg}_{nmg,1} \\ \cdots & \cdots & \cdots \\ L^{bg}_{1,nmb} & \cdots & L^{bg}_{nmg,nmb} \end{bmatrix}_{nmb \times nmg}$$

H_{24} = Coupling coefficients representing the effect of acoustic pressure of the enclosure on the structural response on panel ‘b’

$$= S_b \begin{bmatrix} L^{be}_{1,1} & \cdots & L^{be}_{nme,1} \\ \cdots & \cdots & \cdots \\ L^{be}_{1,nmb} & \cdots & L^{be}_{nme,nmb} \end{bmatrix}_{nmb \times nme}$$

H_{31} = Coupling coefficients representing the effect of the structural vibration of panel ‘a’ on the cavity pressure

$$= \frac{\rho_g c_g^2 S_a \omega^2}{V_g} \begin{bmatrix} \frac{1}{M_{g,1}} \left[L^{ag}_{1,1}, \cdots, L^{ag}_{1,nma} \right] \\ \vdots \\ \frac{1}{M_{g,nmg}} \left[L^{ag}_{nmg,1}, \cdots, L^{ag}_{nmg,nma} \right] \end{bmatrix}_{nmg \times nma}$$

H_{32} = Coupling coefficients representing the effect of the structural vibration of panel ‘b’ on the cavity pressure

$$= -\frac{\rho_g c_g^2 S_b \omega^2}{V_g} \begin{bmatrix} \frac{1}{m_{g,1}} \left[L^{bg}_{1,1}, \cdots, L^{bg}_{1,nmb} \right] \\ \vdots \\ \frac{1}{m_{g,nmg}} \left[L^{bg}_{nmg,1}, \cdots, L^{bg}_{nmg,nmb} \right] \end{bmatrix}_{nmg \times nmb}$$

H_{33} = Modal dynamic stiffness of the gap cavity

$$= \begin{bmatrix} \ddots & & \\ & \left[\omega^2_{g,l} + 2i\zeta_{g,l}\omega_{g,l}\omega - \omega^2 \right] & \\ & & \ddots \end{bmatrix}_{nmg \times nmg}$$

H_{42} = Coupling coefficients representing the effect of the structural vibration of panel ‘b’ on the enclosure pressure

$$= \frac{\rho_e c_e^2 S_b \omega^2}{V_e} \begin{bmatrix} \frac{1}{M_{e,1}} \left[L^{be}_{1,1}, \cdots, L^{be}_{1,nmb} \right] \\ \vdots \\ \frac{1}{M_{e,nme}} \left[L^{be}_{nme,1}, \cdots, L^{be}_{nme,nmb} \right] \end{bmatrix}_{nme \times nmb}$$

H_{44} = Modal dynamic stiffness of the enclosure

$$= \begin{bmatrix} \ddots & & \\ & \left[\omega_{e,n}^2 + 2i\zeta_{e,n}\omega_{e,n}\omega - \omega^2\right] & \\ & & \ddots \end{bmatrix}_{nme \times nme}$$

Modal responses are expressed as,

$$\begin{Bmatrix} \tilde{q}_a \\ \tilde{q}_b \\ \tilde{p}_g \\ \tilde{p}_e \end{Bmatrix} = \begin{bmatrix} H_{11} & 0 & H_{13} & 0 \\ 0 & H_{22} & H_{23} & H_{24} \\ H_{31} & H_{32} & H_{33} & 0 \\ 0 & H_{42} & 0 & H_{44} \end{bmatrix}^{-1} \begin{Bmatrix} F_a \\ 0 \\ 0 \\ 0 \end{Bmatrix} \tag{2.51}$$

2.3.7 Energy transmission parameters

Energy transmission parameters can be written as similar to derived earlier for single wall model,

$$\text{Averaged quadratic velocity } \langle \mathbf{V^2} \rangle = \begin{cases} \frac{\omega^2}{2S_a} \int_{S_a} w_a w_a^* ds & \text{for panel a} \\ \frac{\omega^2}{2S_b} \int_{S_b} w_b w_b^* ds & \text{for panel b} \end{cases} \tag{2.52}$$

where, w_a^* = conjugate of displacement of panel ‘a’

w_b^* = conjugate of displacement of panel ‘b’

Acoustic energy transmitted to the gap cavity as well as enclosure, is quantified using averaged sound pressure level of the air gap$L_{p,g}$ and the averaged sound pressure level of the enclosure$L_{p,e}$. Averaged sound pressure level is a measure of averaged quadratic pressure with respect to square of reference sound pressure. Averaged sound pressure level of the gap cavity and the enclosure are formalized in Eq. (2.53) to Eq. (2.56).

$$L_{p,g} = 10\log\left(\langle P_g^2 \rangle / P_{ref}^2\right) \tag{2.53}$$

$$\langle P_g^2 \rangle = \frac{1}{2V_g} \int_{V_g} P_g P_g^* dv \tag{2.54}$$

where, Reference pressure,P_{ref} = 20 μPa.

P_g^* = Complex conjugate of the acoustic pressure in the gap cavity.

$$L_{p,e} = 10\log\left(\langle P_e^2 \rangle / P_{ref}^2\right) \tag{2.55}$$

$$\langle P_e^2 \rangle = \frac{1}{2V_e} \int_{V_e} P_e P_e^* dv \tag{2.56}$$

P_e^* = Complex conjugate of the acoustic pressure in the enclosure.

For energy transmission mechanism through semi-cylindrical single and double wall panel, separate programs are developed using MATLAB platform. The free vibration results, i.e. mesh data, natural frequencies, mode shapes etc., of the structural and acoustic components are obtained from ANSYS (ver. 11) and are exported into MATLAB program. Based on the developed numerical model, some case studies are performed and are detailed in the next chapter.

CHAPTER 3: RESULTS AND DISCUSSIONS

The developed coupled vibro-acoustic model as presented in the earlier chapter is validated for energy transmission through double wall flat panels. Once the developed formulation is validated, energy transmission characteristics of a semi-cylindrical single wall curved panel with different varying parameters, i.e. loading case, damping co-efficient, thickness of panel, laminated composite panel etc. are studied. Subsequently, using the developed double wall vibro-acoustic model, energy transmission characteristics through double wall structure is studied. The results and observations are detailed in the next few sections.

3.1. Validation for Energy Transmission through Flat Double-Wall Panel

In this subsection the developed numerical model for energy transmission through a double wall flat panel is validated with Cheng et al [37]. The schematic diagram of the flat double wall model is shown in Figure 3.1.

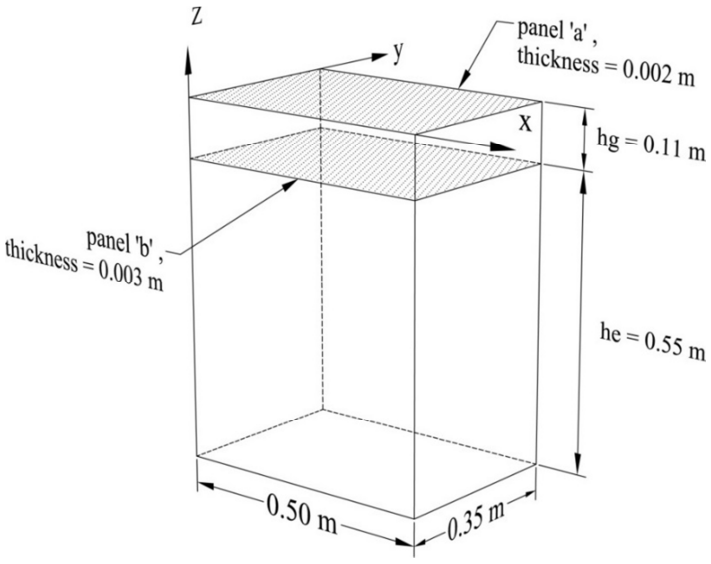

Figure 3.1: Model of the double wall flat structure connected to an enclosure

Thickness of gap cavity is denoted by h_g and thickness of the enclosure is denoted by h_e. In this case h_g/h_e =0.2. Both the panels ‘a’ and ‘b’ are assumed to be made of aluminium. The panels are assumed as simply supported along all the edges. A harmonic loading of magnitude 1 N is applied at (0.2m, 0.14m) on panel ‘a’. Modal loss factors are assumed as 0.005 for panels and 0.001 for the gap cavity and the enclosure.

Averaged quadratic velocity for both the panels are calculated from the developed model and plotted in Figure 3.2 and the averaged sound pressure levels in the air gap and enclosure for double wall flat panel plotted in Figure 3.3.

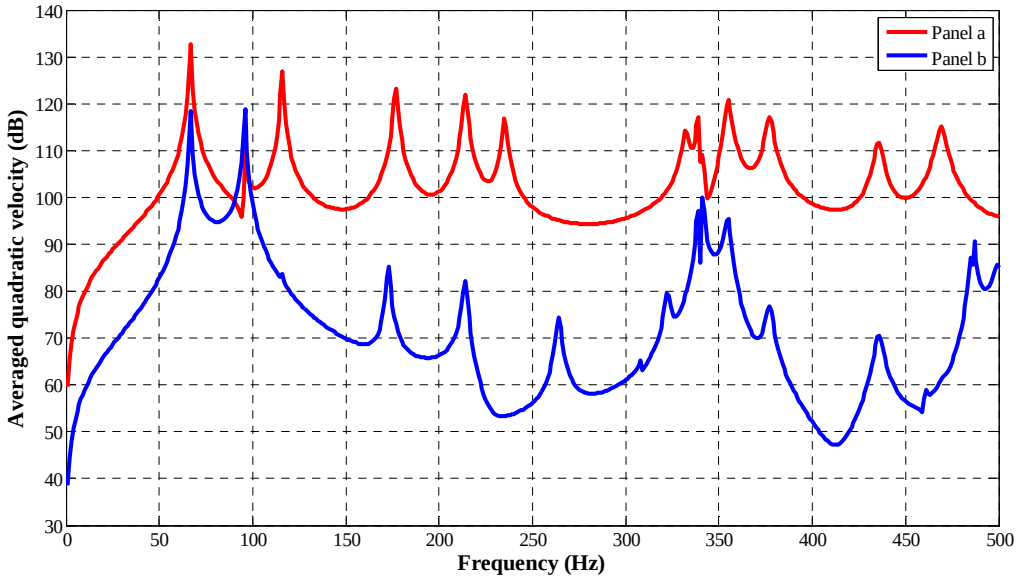

Figure 3.2: Averaged quadratic velocity of double wall flat panel (present model) (h_g/h_e=0.2)

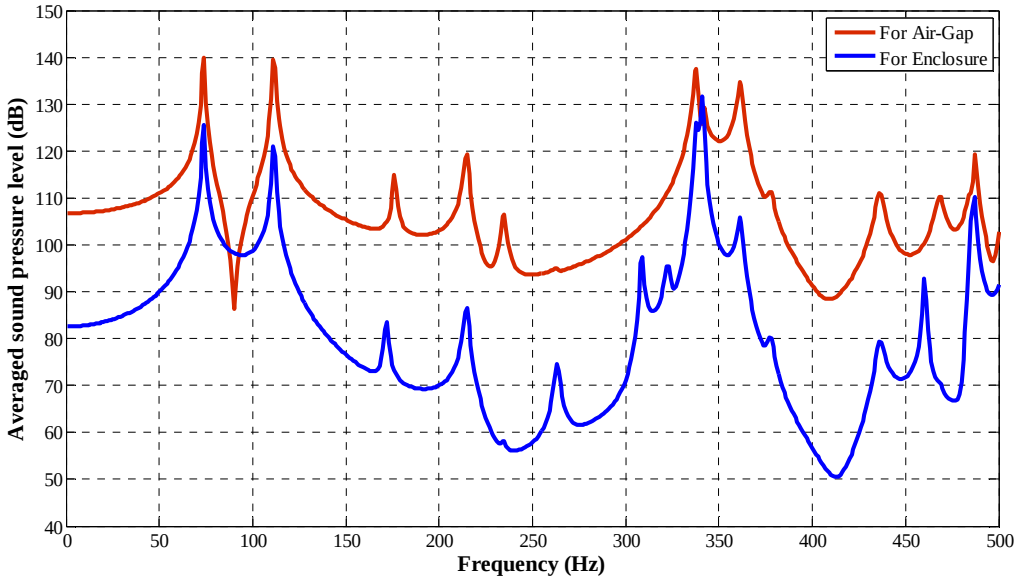

Figure 3.3: Averaged sound pressure level in gap-cavity and enclosure for double wall flat panel (present model) (h_g/h_e=0.2)

Averaged quadratic velocity of both the panels also averaged sound pressure levels in the air gap and enclosure for double wall panel with same properties as considered above in present model, were present in research article by Cheng et al [37], which are present in Figure 3.4

and 3.5 respectively. It is observed that the obtained results from the present mathematical model compare reasonably well with those reported in the article by Cheng et al.

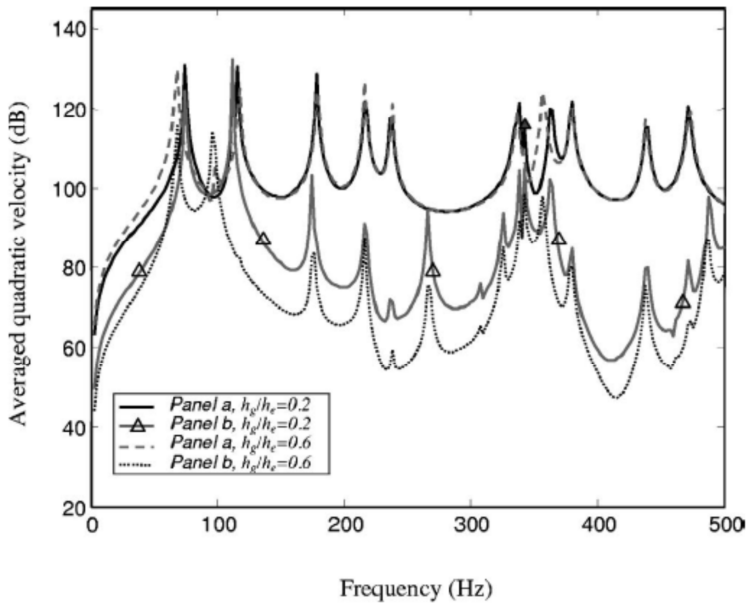

Figure 3.4: Averaged quadratic velocity of the panels of double wall flat panel (Figure 5(a), Cheng et al [37])

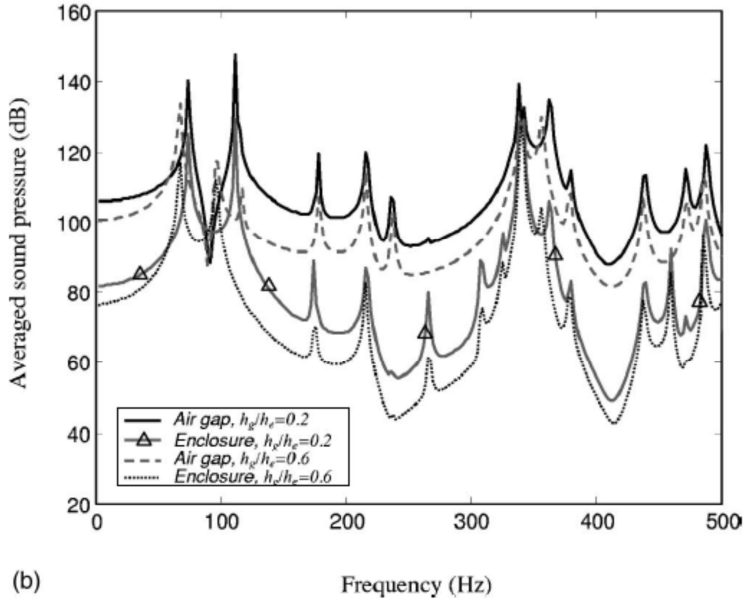

Figure 3.5: Averaged sound pressure level inside the air gap and the enclosure of double wall flat panel (Figure 5(b), Cheng et al [37])

Table 3.1: Comparison of averaged quadratic velocity of the panels from Present flat plate model with Cheng et al results

Panel 'a'			Panel 'b'		
Freq. (Hz)	Averaged quadratic velocity (dB)		Freq. (Hz)	Averaged quadratic velocity (dB)	
	Present model	Cheng et al. [37]		Present model	Cheng et al. [37]
74	130.5	131	74	124.2	125
115	126.7	128	111	123.1	132
176	123.5	125	172	97	102
215	121	121	215	90.4	91
235	116.4	117	235	73.27	73
337	119.7	121	337	102.1	103
362	118.7	120	361	101.4	102
378	116.9	118	377	81.2	84
436	112	114	436	77.5	79
468	115.1	118	468	77	82

Table 3.2: Comparison of averaged sound pressure level of the air gap and the enclosure from Present flat plate model with Cheng et al results

Air Gap			Enclosure		
Freq. (Hz)	Averaged sound pressure (dB)		Freq. (Hz)	Averaged sound pressure (dB)	
	Present model	Cheng et al. [37]		Present model	Cheng et al. [37]
74	140	140	74	125.5	125
111	139.4	145	111	121	126
176	114.9	118	172	83.6	88
215	119.2	120	215	86.6	87
235	106.5	106	236	74.5	78
338	137.5	138	341	131.7	132
361	134.7	135	361	105.9	106
436	111.1	113	436	79.3	81
468	110.2	114	460	92.8	93
487	119.3	121	487	110.3	102

3.2 Sound Transmission through Semi-cylindrical Single wall panel

3.2.1 Model Properties

In the present study a Semi-cylindrical Single wall panel (Panel 's') connected to a semi-cylindrical enclosure (defined by a subscript 'e') is modelled. The panel is considered as simply supported along all edges. The panel is excited by different external excitations and the sound transmission characteristics are observed. A total number of four cases are studied by varying the external excitation, damping property of the system, thickness of panel, and properties of the panel.

The geometric properties in different cases of Semi-cylindrical single wall panel are stated below:

i. Length of the model (L) : 2 m
ii. Radius of the model (R) : 0.2 m
iii. The thickness of the panel : 2 mm (in Case 1, Case 2 and Case 4)

4mm (in Case 3)

In Case 1 to Case 3, the aluminum panel is considered and in Case 4 different laminated composite panel is considered in the model. The material properties of aluminum, which are considered in the model is listed in the Table 3.3. The material properties of laminated composites are given later.

Table 3.3: Material properties of Aluminum used in case studies

Modulus of Elasticity	70 GPa
Poisson's ratio	0.3
Density	2700 kg/m3

The properties of fluid in enclosure is same for all Cases, which are listed in Table 3.4.

Table 3.4: Material properties of fluid in enclosure used in case studies

Density	1.204 kg/m3
Speed of sound	340 m/s

The damping properties considered in the Case studies are given in Table 3.5.

Table 3.5: Damping Co-efficients used in case studies

	Structural Damping	Acoustic Damping
Case 1	0.0 %	0.0
Case 2	0.0, 0.1 and 0.5 %	0.0, 0.1 and 0.5 %
Case 3 and Case4	0.0 and 0.5 %	0.0 and 0.5 %

3.2.2 Case Study-1: Effect of Different loading on Sound Transmission through Single wall

In this sub-section, different loading cases are considered on semi-cylindrical single wall panel at different loading position or orientation. The response parameters, i.e. averaged quadratic velocity $<V^2>$ and averaged sound pressure level <p>, are studied in detail to understand the energy transmission characteristics of the coupled system with the various loading cases. The loading cases that are considered in the study are point load, patch load and pressure load.

3.2.2.1 Effect of Point Load Variation

Harmonic response analysis based on the present mathematical formulation is carried out in the low frequency region limited up to 500 Hz. A harmonic point load of magnitude 1 N is applied normal to the surface of panel at different location over a frequency range of 1-500 Hz and modal responses are evaluated using Eq. (2.24). Once the frequency responses are obtained from modal domain, total responses are computed and the averaged quadratic

velocities $<V^2>$ in dB for the panel and averaged sound pressure level <p> in dB for the enclosure are plotted.

Now this external point load excitation is shifted along the crown as shown in Figure 3.6, on three locations as listed in Table 3.6 to understand the response behaviour of the coupled system for point load variation along the crown. Averages quadratic velocity of the panel and Averages sound pressure level (dB) in the enclosure for these point load excitation calculated from developed numerical model, are given in Figure 3.7 and Figure 3.8.

Table 3.6: Detail of loading applied for longitudinally shifting of point load excitation

Loading Case	PT-1,1	PT-1,2	PT-1,3
Co-ordinate of Loading Point	(0,0.2,0.5)	(0,0.2,1.0)	(0,0.2,1.5)

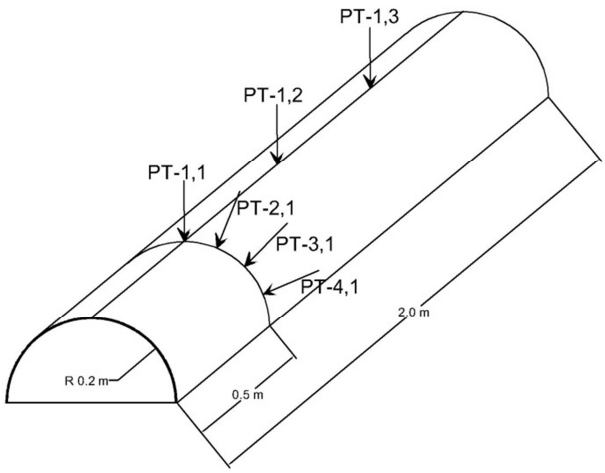

Figure 3.6: Schematic model for Semi-cylindrical single wall subject to Point Load at various loading point.

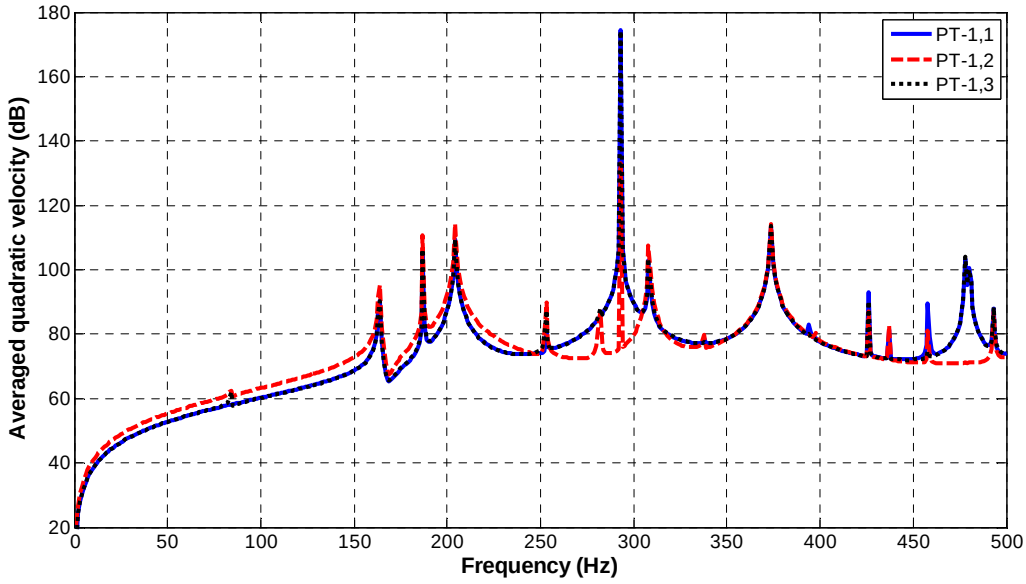

Figure 3.7: Average quadratic velocity of the panel subjected to point load excitation shifting longitudinally along the crown

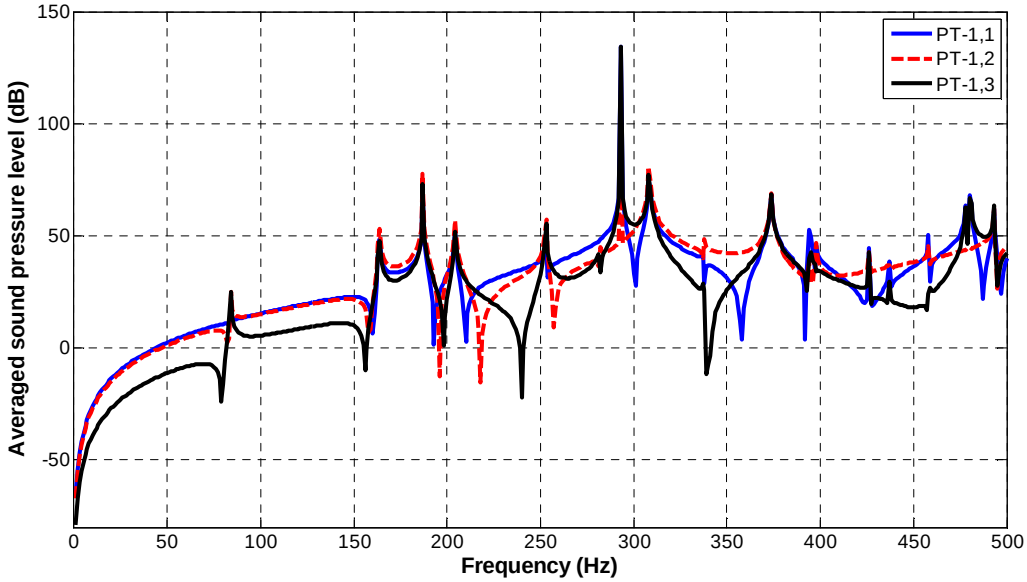

Figure 3.8: Average sound pressure level (dB) in enclosure subjected to point load excitation shifting longitudinally along the crown

The obtained $<V^2>$ plot for these point load excitation as shown in Figure 3.8 are presented in a tabular form in Table 3.7. The modes dominated by the panel and cavity are present separately from better understanding of the coupled system.

Table 3.7: Comparison of averages quadratic velocity of panel for point load excitation shifting longitudinally along the crown

Panel Dominated Modes					Cavity Dominated Modes				
Uncoupled Frequency in Hz (mode shape no.)	Coupled Case				Uncoupled Frequency in Hz (mode shape no.)	Coupled Case			
	Coupled Freq. in Hz	Avg. Quad. Velocity (dB)				Coupled Freq. in Hz	Avg. Quad. Velocity (dB)		
		Loading Case PT-1,1	Loading Case PT-1,2	Loading Case PT-1,3			Loading Case PT-1,1	Loading Case PT-1,2	Loading Case PT-1,3
186.45(4,1)	187	105.30	110.70	106.40	0.00(0,0,0)	-	-	-	-
199.08(3,1)	204	109.60	114.50	109.50	85.02(0,0,1)	83	-	62.16	60.24
281.79(4,2)	282	-	87.00	88.04	170.17(0,0,2)	164	90.63	95.35	90.27
292.99(5,2)	293	174.30	133.20	174.20	255.59(0,0,3)	253	80.37	89.86	87.31
307.82(5,1)	308	102.70	107.70	103.60	341.40(0,0,4)	338	78.90	79.89	-
373.79(5,3)	374	113.60	114.20	113.60	427.74(0,0,5)	426	92.90	87.05	90.28
393.51(7,2*)	394	83.09	80.30	-	498.36(1,0,0)	493	87.91	87.11	88.28

399.13(6,3)	398	-	-	-	
437.11(6,2)	437	81.42	82.64	73.13	
463.90(5,2)	458	89.41	81.20	74.64	
480.17(5,4)	478	103.40	-	104.00	
482.13(6,4)	480	100.50	-	100.10	

In the next set of analysis, external point load excitation is shifted radially at z = 0.5, on four location as listed in Table 3.8. Average quadratic velocities of the panel and Average sound pressure level (dB) in enclosure subjected to these point load excitation are given in Figure 3.9 and Figure 3.10.

Table 3.8: Detail of loading applied for radially shifting of point load excitation

Loading Case	PT-1,1	PT-2,1	PT-3,1	PT-4,1
Co-ordinate	(0,0.2,0.5)	(0.077,0.185,0.5)	(0.141,0.141,0.5)	(0.185,0.077,0.5)
Angle	90°	67.5°	45°	22.5°

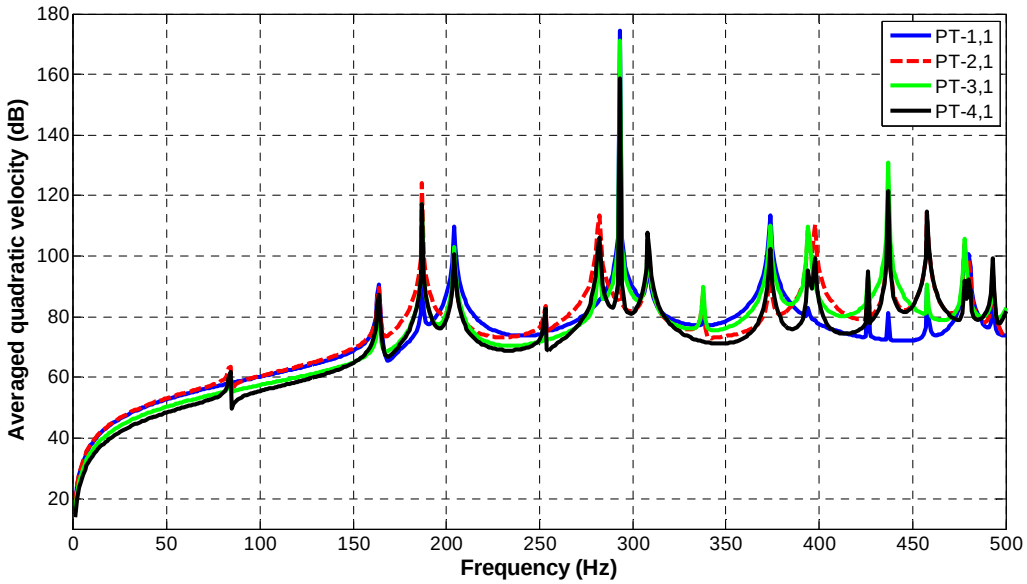

Figure 3.9: Average quadratic velocity of the panel subjected to point load excitation shifting radially along z = 0.5 m

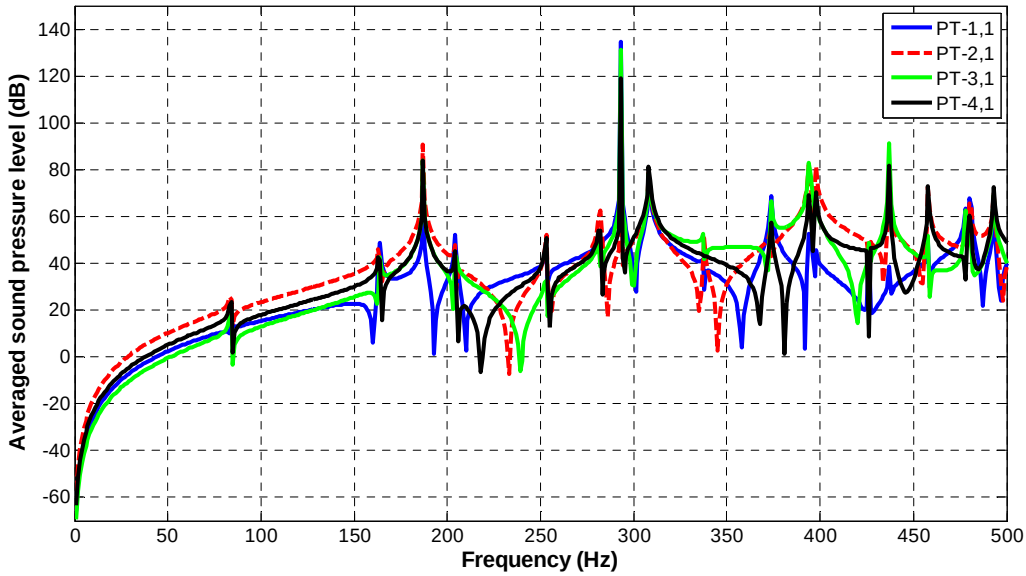

Figure 3.10: Average sound pressure level (dB) in enclosure subjected to point load excitation shifting radially along z = 0.5 m

The obtained $<V^2>$ plot for point load excitation shifting radially along z = 0.5 m as shown in Figure 3.9 are presented as tabular form in Table 3.9.

Table 3.9: Comparison of average quadratic velocity of the panel subjected to point load excitation shifting radially along z = 0.5 m

Panel Dominated Modes						Cavity Dominated Modes					
Uncoupled Frequency in Hz (mode shape no.)	Coupled Case					Uncoupled Frequency in Hz (mode shape no.)	Coupled Case				
	Coupled Freq. in Hz	Avg. Quad. Velocity (dB)					Coupled Freq. in Hz	Avg. Quad. Velocity (dB)			
		Loading Case PT-1,1	Loading Case PT-2,1	Loading Case PT-3,1	Loading Case PT-4,1			Loading Case PT-1,1	Loading Case PT-2,1	Loading Case PT-3,1	Loading Case PT-4,1
186.45(4,1)	187	105	124	117	117	0.00(0,0,0)	-	-	-	-	-
199.08(3,1)	204	110	101	103	101	85.02(0,0,1)	83	-	63	59	62
281.79(4,2)	282	-	113	98	106	170.17(0,0,2)	164	91	90	83	87
292.99(5,2)	293	174	145	171	159	255.59(0,0,3)	253	80	83	74	83
307.82(5,1)	308	103	106	105	108	341.40(0,0,4)	338	79	88	90	-
373.79(5,3)	374	114	97	110	102	427.74(0,0,5)	426	93	93	94	95
393.51(7,2*)	394	83	108	110	95	498.36(1,0,0)	493	88	96	96	99
399.13(6,3)	398	-	110	-	100						

437.11(6,2)	437	81	122	131	122
463.90(5,2)	458	89	114	91	115
480.17(5,4)	478	103	104	106	92
482.13(6,4)	480	101	99	-	92

To predict the maximum energy transmission through the panel for the different loading case from average quadratic velocity and average sound pressure level as shown in Figure 3.7 to Figure 3.10, is a bit difficult. So, 1/3 Octave plot for average sound pressure level are calculated with the help of data obtained from developed numerical model. Octave plot for average sound pressure subjected to different point load excitation shifted longitudinally along the crown and shifted radially along z = 0.5 m are given in Figure 3.11 and Figure 3.12 respectively. The frequencies of 1/3 octave band are given in Table 3.10.

Table 3.10: Frequencies of 1/3 octave band

Lower Cutoff Frequency (in Hz)	Center Frequency (in Hz)	Upper Cutoff Frequency (in Hz)
0.9	1	1.1
1.1	1.25	1.4
1.4	1.6	1.8
1.8	2	2.2
2.2	2.5	2.8
2.8	3.15	3.5
3.5	4	4.5
4.5	5	5.6
5.6	6.3	7.1
7.1	8	9.0
9.0	10	11.2
11.2	12.5	14.1
14.1	16	17.8
17.8	20	22.4
22.4	25	28.2
28.2	31.5	35.5
35.5	40	44.7
44.7	50	56.2
56.2	63	70.8
70.8	80	89.1
89.1	100	112.0
112.0	125	141.0
141.0	160	178.0
178.0	200	224.0
224.0	250	282.0
282.0	315	355.0
355.0	400	447.0
447.0	500	562.0

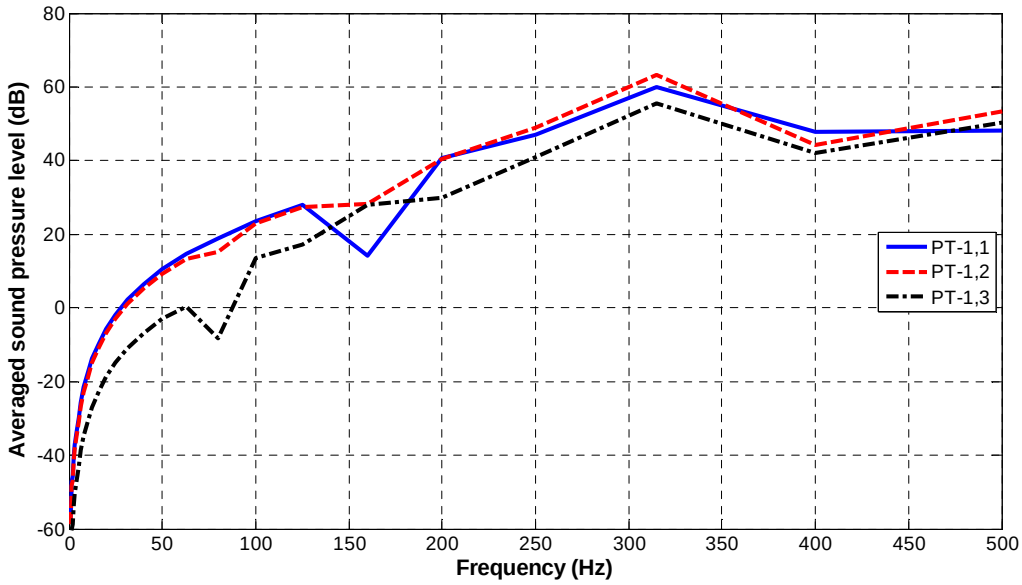

Figure 3.11: Octave plot of average sound pressure level (dB) in enclosure subjected to different point load excitation shifted longitudinally along the crown

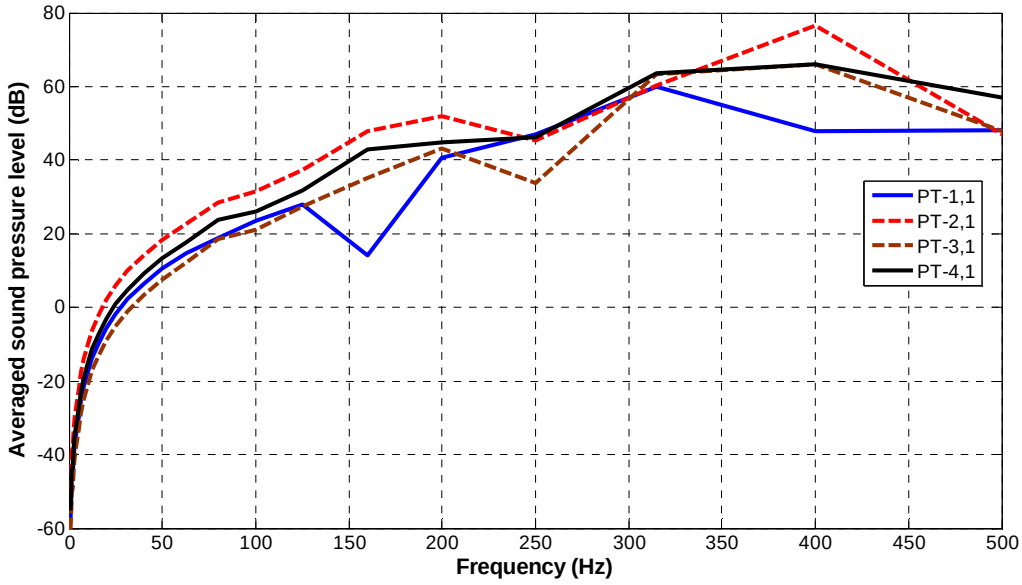

Figure 3.12: Octave plot of average sound pressure level (dB) in enclosure subjected to different point load excitation shifted radially along z = 0.5 m

Similar analysis is done for point load variation longitudinally along the 67.5°, 45° and 22.5° and radially along z = 1.0 m and z = 1.5 m. The results of this study are not given in this thesis to make presentation compact.

Some of the observations made from the above results are:

i) Energy transmission characteristics are dominated by the modes that are dominated by the panel and enclosure has only little effect on averaged quadratic velocities of the panel.

ii) Maximum response occurs at 293 Hz coupled frequency in all case, but this huge response occurs due to some singularity problem at this particular frequency. If the structural damping is slightly increased to 0.1 %, singularity problem can be mitigated and response at this particular frequency will decrease very significantly. This singularity problem is discussed in detail in next sub-section. However, this maximum response is ignored as this is due to some numerical error.

iii) For uncoupled case, one can say the response will be on the high side at a particular frequency if the load is applied at antinodes of corresponding mode shape obtained from free vibration anlysis. Whereas, for coupled case the mode shape cannot be predicted from free vibration data, a proper vibro-acoustic model is required.

iv) The structural panel is symmetrical about middle plan (z=1.0) inspite of that the response of the load case PT-1,1 and PT-1,3 is not similar. From this it can be concluded that, inspite of symmetrical boundary conditions and other structural parameters (like configuration, mode shape, etc.) the response behaviour of coupled case will not similar for symmetrical loading.

v) From the Octave plot showed in Figure 3.11 and Figure 3.12, it is clear that the maximum sound energy transmission occurs for loading case PT-2,1 (0.077,0.185,0.5) or (θ=67.5° and z = 0.5m).

3.2.2.2 Effect of Patch Load Variation

In the previous sub-section, point load is applied on semi-cylindrical single wall panel at different locations and sound transmission behavior is studied for various loading position of point load. In the present sub-section patch load is applied instead of point load and loading positions are varied on the surface of the panel, as shown in Figure (3.13) . The size of the patch is 0.25 m by 0.1 m.

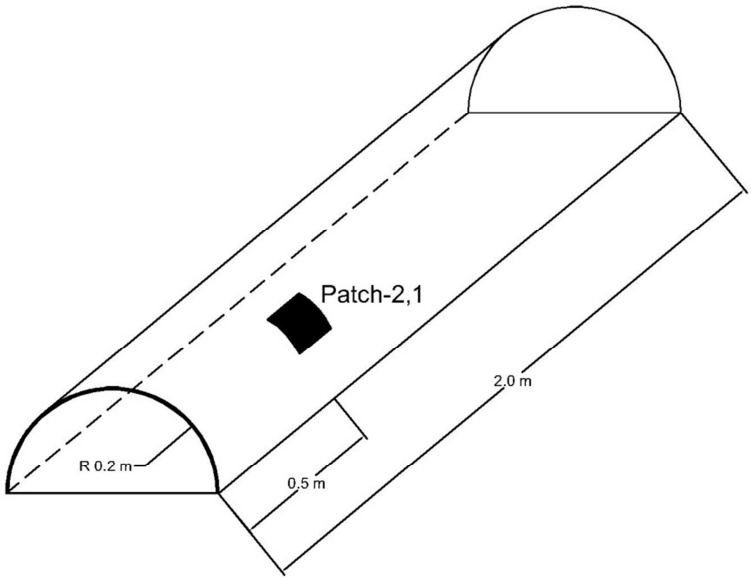

Figure 3.13: Schematic model for Semi-cylindrical single wall subject to Patch Load

Now this external patch load excitation is shifted along the crown, for three locations as listed in Table 3.11 to understand the response behavior of coupled system for patch load variation along the crown similar to point load case discussed in earlier. Averages quadratic velocity of panel and averages sound pressure level (dB) in enclosure for different position of patch load excitation calculated from developed numerical model and given in Figure 3.14 and Figure 3.15.

Table 3.11: Detail of loading applied subjected to point load excitation shifted longitudinally

Loading Case	Patch-1,1	Patch-1,2	Patch-1,3
Co-ordinate Centre of Patch	(0,0.2,0.5)	(0,0.2,1.0)	(0,0.2,1.5)

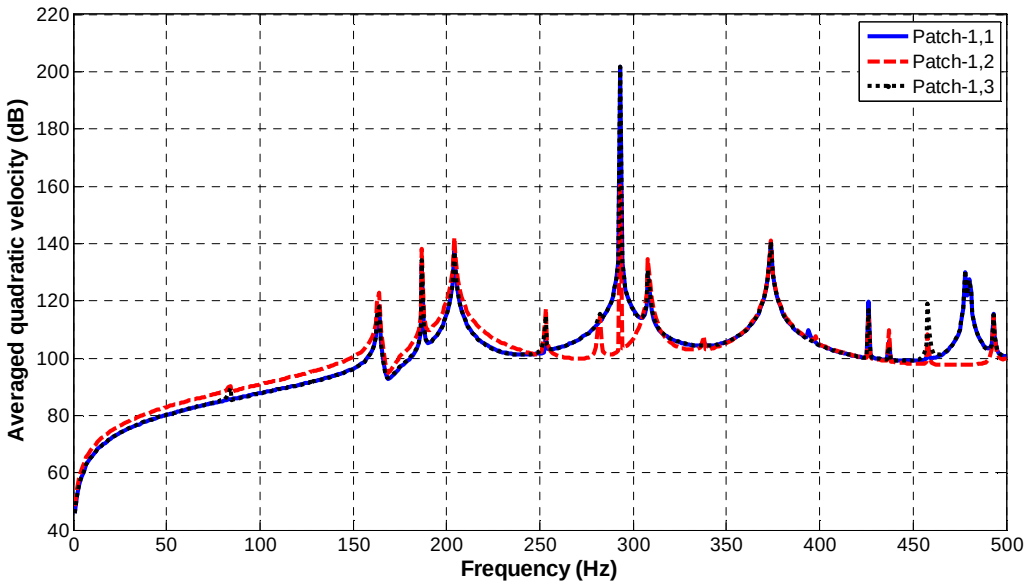

Figure 3.14: Average quadratic velocity of the panel subjected to patch load excitation shifted longitudinally along the crown

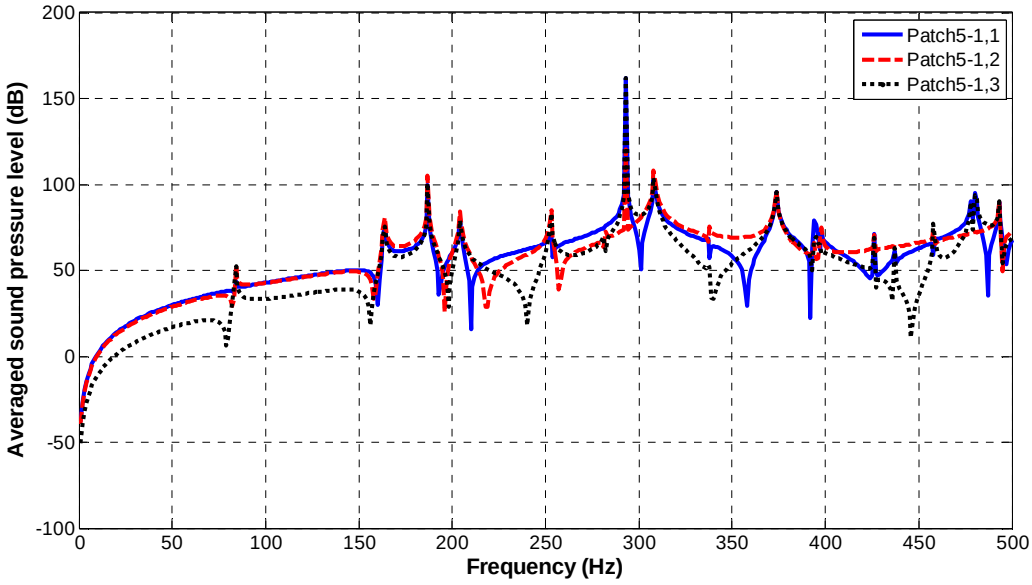

Figure 3.15: Average sound pressure level (dB) in enclosure subjected to patch load excitation shifted longitudinally along the crown

Some of the observations made from the above results are:

i) It is mentioned in previous sub-section for point load excitation the response is not symmetrical for Loading case PT-1,1 and PT-1,3 which are symmetrical loading cases. But for patch load a different observation is noticed. The velocity response of Patch-1,1 and Patch-1,3 is similar. So, it can be concluded that if the structural parameters are symmetrical, the structural response will be similar for symmetrical loading patch loading.

ii) There is a lot of difference in the pressure responses for Loading case Patch-1,1 and Pacth-1,3. The cavity modes are not symmetrical in the longitudinal axis which is the root cause of this phenomena.

iii) The overall sound transmission behaviour (both structural response and pressure response) of semi-cylindrical single wall model subjected to patch load and point load is similar.

3.2.2.3 Effect of Pressure Load Variation

In this sub-section, pressure load is applied on the semi-cylindrical single wall panel at different incident angle. The response parameters, i.e. averaged quadratic velocity $\langle V^2 \rangle$ and averaged sound pressure level <p> are obtained from developed numerical model.

Pressure load is applied on the structural panel at a certain angle with the horizontal plane. The angle of incident pressure load is varied. Four incident angles are considered in the present analysis, i.e. 22.5°, 45°, 67.5° and 90°. Average quadratic velocity of the panel and average sound pressure level (dB) in the enclosure for different incident pressure are calculated from developed numerical model and given in Figure 3.16 and Figure 3.17 respectively.

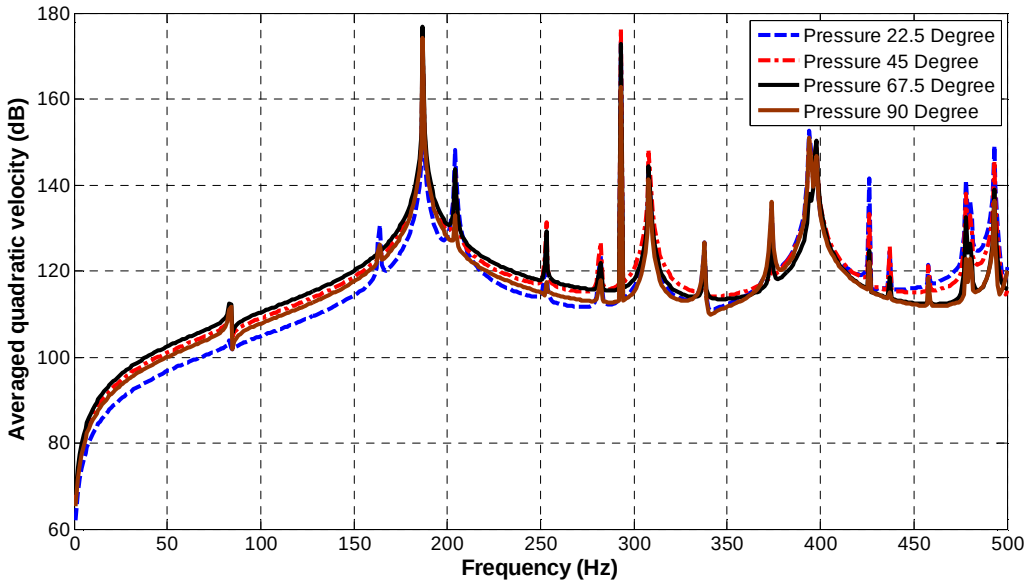

Figure 3.16: Average quadratic velocity of panel subjected to pressure load excitation at different incident angle

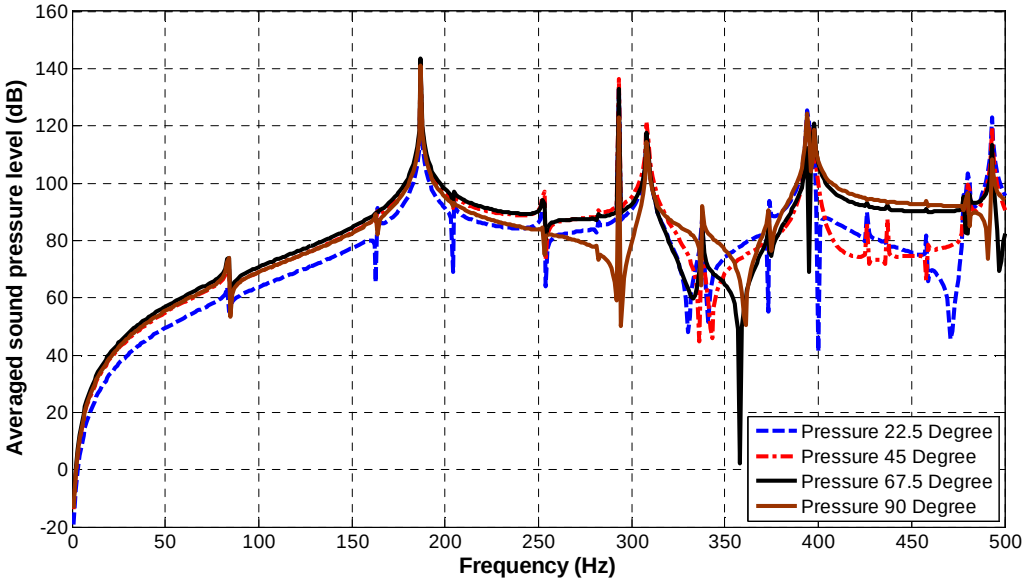

Figure 3.17: Average sound pressure level (dB) in enclosure subjected to pressure load excitation at different incident angle

Some of the observations made from the above results are:

i) From pressure plot, it is clear that the sound pressure level inside the enclosure at 90° and 67.5° incident pressure load is much greater than that of 45° and 22.5° incident pressure load. And maximum sound pressure inside the enclosure is observed for 90° incident pressure load. When incident angle is closed to 90° more surface area of the panel is subjected to external loading, which causes more pressure inside the enclosure.

ii) For velocity response, a different behaviour is noticed. At different frequency, different incident angle is causing the maximum velocity response. The behaviour of the velocity response can be understand is the help of coupled mode shape as discussed for point load and patch load excitation.

3.2.3 Case Study-2: Effect of damping on Sound Transmission through Single wall

In previous sub-section all studies are carried out on a system with the zero structural and cavity damping. In the present section, a study is carried out to understand the effect of structural and cavity damping on the response of vibro-acoustically coupled system.

The response is calculated from the developed numerical model of the coupled system with various damping co-efficient for structure and acoustics, which are given in the Table 3.12.

Table 3.12: Damping Co-efficient considered in different cases of Single Wall panel

Case No.	D1	D2	D3	D4	D5
Structural Damping	0%	0.1%	0.5%	0%	0%
Acoustic Damping	0%	0%	0%	0.1%	0.5%

In the previous sub-section it is shown that for single subjected to point load at different location on the semi-cylindrical panel, the response is maximum for PT-2,1 loading case. Therefore, the response of the coupled system for different damping case as mentioned above for the point load excitation applied at z = 0.5m and theta 67.5° (this loading case is referred as 'PT-2,1') are evaluated. Two cases considered in this section. In first case, the acoustics damping is kept at 0% and the structural damping taken as 0%, 0.1% and 0.5% to understand the effect of increase of structural damping with 0% acoustics damping and averaged quadratic velocity plot is given in Figure 3.18 and also a tabular form of this velocity response is given in Table 3.13.

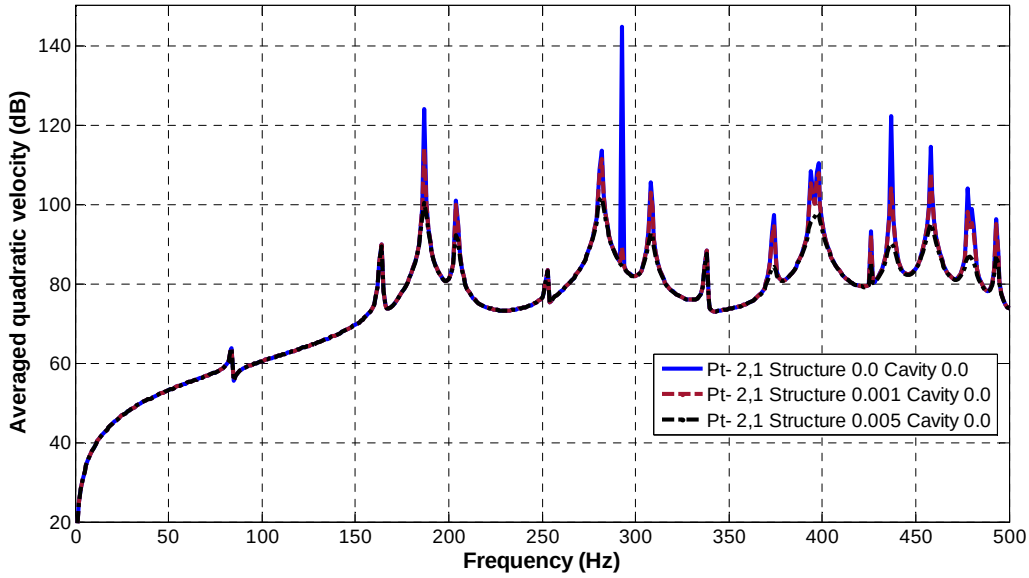

Figure 3.18: Averages quadratic velocity of the panel for Loading Case PT-2,1 for different structural damping with zero acoustics damping

Table 3.13: Comparison of averages quadratic velocity of panel for Loading Case PT-2,1 for different structural damping with zero acoustics damping

Panel Dominated Modes					Cavity Dominated Modes				
Uncoupled Frequency in Hz (mode shape no.)	Coupled Case				Uncoupled Frequency in Hz (mode shape)	Coupled Case			
	Coupled Freq. in Hz	Avg. Quad. Velocity (dB)				Coupled Freq. in Hz	Avg. Quad. Velocity (dB)		
		Case D1 (ξs= 0% & ξa = 0%)	Case D2 (ξs= 0.1% & ξa = 0%)	Case D3 (ξs= 0.5% & ξa = 0%)			Case D1 (ξs= 0% & ξa = 0%)	Case D2 (ξs= 0.1% & ξa = 0%)	Case D3 (ξs= 0.5% & ξa = 0%)
186.45(4,1)	187	124.1	114	100.500	0.00(0,0,0)	-	-	-	-
199.08(3,1)	204	100.8	99.79	92.190	85.02(0,0,1)	84	63.250	63.620	63.62
281.79(4,2)	282	113.4	111.5	101.700	170.17(0,0,2)	164	89.790	89.770	89.360
292.99(5,2)	293	144.7	88.98	-	255.59(0,0,3)	253	83.540	83.520	83.270
307.82(5,1)	308	105.5	103.1	92.630	341.40(0,0,4)	338	88.240	88.210	87.480
373.79(5,3)	374	97.38	94.44	84.300	427.74(0,0,5)	426	93.250	92.220	85.290
393.51(7,2*)	394	108.3	105.2	-	498.36(1,0,0)	493	96.160	94.990	85.930
399.13(6,3)	398	110.3	107.9	97.690					
437.11(6,2)	437	122.3	103.9	90.200					
463.90(5,2)	458	114.4	107.8	94.890					
480.17(5,4)	478	103.9	98.03	86.79 (At 479 Hz)					
482.13(6,4)	480	98.74	95.21						

In next case, the structural damping is kept at 0% and the acoustics damping taken as 0%, 0.1% and 0.5% to understand the effect of increase of acoustics damping with 0% structural damping and averaged quadratic velocity plot is given in Figure 3.19 and also a tabular form of this velocity response is given in Table 3.14.

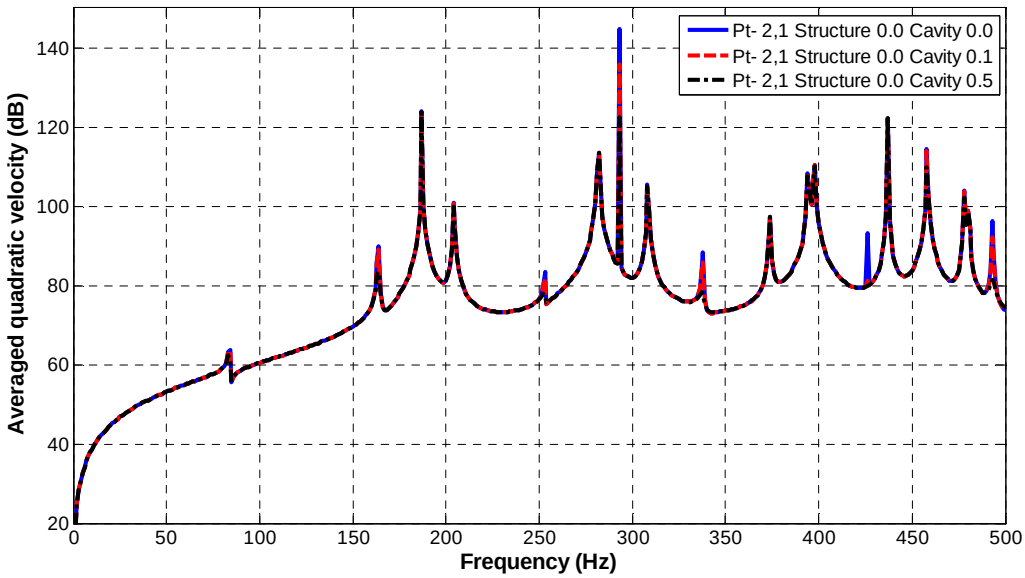

Figure 3.19: Averages quadratic velocity of panel for Loading Case PT-2,1 for different acoustics damping

Table 3.14: Comparison of averages quadratic velocity of panel for Loading Case PT-2,1 for different acoustics damping

Panel Dominated Modes	Cavity Dominated Modes

Uncoupled Frequency in Hz (mode shape no.)	Coupled Case				Uncoupled Frequency in Hz (mode shape no.)	Coupled Case			
	Coupled Freq. in Hz	Avg. Quad. Velocity (dB)				Coupled Freq. in Hz	Avg. Quad. Velocity (dB)		
		Case D1 (ξs= 0% & ξa = 0%)	Case D4 (ξs= 0% & ξa = 0.1%)	Case D5 (ξs= 0% & ξa = 0.5%)			Case D1 (ξs= 0% & ξa = 0%)	Case D4 (ξs= 0% & ξa = 0.1%)	Case D5 (ξs= 0% & ξa = 0.5%)
186.45(4,1)	187	124.1	124.10	123.80	0.00(0,0,0)	-	-	-	-
199.08(3,1)	204	100.8	100.70	99.47	85.02(0,0,1)	84	63.250	63.35	62.51
281.79(4,2)	282	113.4	113.40	113.40	170.17(0,0,2)	164	89.790	89.19	83.35
292.99(5,2)	293	144.7	135.80	122.30	255.59(0,0,3)	253	83.540	81.59	77.72
307.82(5,1)	308	105.5	105.50	105.10	341.40(0,0,4)	338	88.240	85.72	78.33
373.79(5,3)	374	97.38	97.38	97.37	427.74(0,0,5)	426	93.250	81.17	-
393.51(7,2*)	394	108.3	108.30	107.60	498.36(1,0,0)	493	96.160	92.09	81.43
399.13(6,3)	398	110.3	110.30	110.20					
437.11(6,2)	437	122.3	122.30	122.20					
463.90(5,2)	458	114.4	114.10	109.90					
480.17(5,4)	478	103.9	103.80	102.20					
482.13()	480	98.74	98.78	98.60					

From above some observations may be summarized as follows:

a) For the structure dominating modes, the velocity response decreases significantly with the increase of structural damping, whereas decrease in response is observed with the increase of cavity damping.
b) For the acoustics dominating modes, the velocity response decreases with the increase of cavity damping, whereas a very little decrease in response is observed with increase of structural damping.

c) As discussed in previous sub-section at 293 Hz coupled frequency a singularity problem occurred. When structural damping is slightly increased to 0.1% a drastic decrease in response is observed and for 0.5% structural damping the peak of velocity response vanished. This behavior can be explained with help of the Modal dynamic stiffness of structure panel (H11) mentioned in eq. 2.24.For ξ_s=0, co-efficient of the H11 reduced to$\left[\omega_{s,j}^2 - \omega^2\right]$ ignoring the mass term and for ξ_s=0.1% co-efficient of the H11 will be$\left[\omega_{s,j}^2 + i0.002\omega_{s,j}\omega - \omega^2\right]$. These two 'co-efficient of the H11' are listed in Table (3.15) for natural frequency of structural panel and driving frequency. From Table (3.15) it is clear, the change in stiffness term is insignificant for **ξ_s=0% and ξ_s=0.1%** with an exception at 293 Hz frequency. The stiffness term increases about 4 times for **ξ_s=0.1%**.

Table 3.15 Comparison of co-efficient of the H11forξ_s=0 and ξ_s=0.1%

NATURAL FRQ. ($\omega_{s,j}$)	COUPLED FRQ. (ω)	Co-efficient of the H11	
		for ξ_s=0	For ξ_s= 0. 1%
186.449	187.000	205.7749	205.9442
199.076	204.000	1984.802	1984.822
281.789	282.000	119.0361	119.7018
292.993	293.000	4.196881	13.75891
307.815	308.000	113.9042	114.7335
373.792	374.000	155.4092	156.3061
393.515	394.000	382.0683	382.4739
399.133	398.000	903.5029	903.6787
437.113	437.000	98.45043	100.3719
463.904	458.000	5442.518	5442.557
480.168	478.000	2076.916	2077.027
482.133	480.000	2052.278	2052.391

d) The structural velocity decreases with the increase of acoustics damping keeping the structural damping constant, as observed in Table 3.13. This phenomena indicates the effect of acoustic back pressure on the structural panel.

3.2.4 Case Study-3: Effect of thickness on Sound transmission

In this section, effect of increase in thickness in sound transmission is studied semi-cylindrical single wall panel. If thickness of the panel increases, both the mass and stiffness of panel will increase. In the review of past research articles, it is clear that with the increase of mass and stiffness the noise transmission will decrease. In the present study, the effect of increase of thickness on panel is studied by the developed model.

Using the developed model of semi-cylindrical wall panel, the response of structural panel of thickness 4mm and other properties are same as taken in earlier case. The obtained result is compared with the response obtained from earlier model of 2mm thick panel. Two cases are considered, i.e. (i) structural damping 0% and acoustics damping 0% and (ii) structural damping 0% and acoustics damping 0%. The PT-2,1 loading case is considered similar to earlier sub-section. Average quadratic velocity plot are for 4 mm and 2 mm thick panel are given in Figure 3.20 to Figure 3.21 and also presented in tabular form in Table 3.16 to table 3.17.

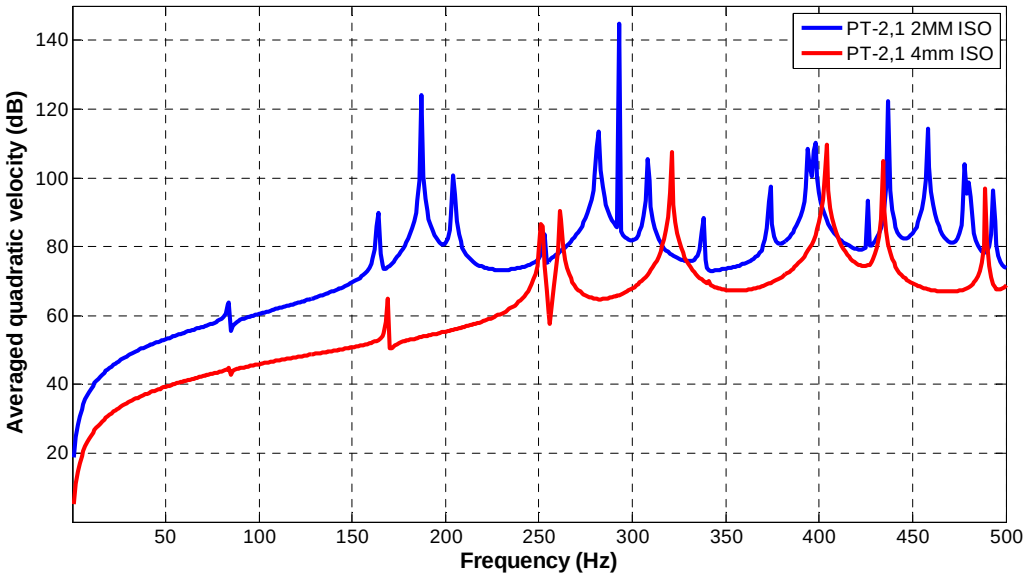

Figure 3.20: Average quadratic velocity of 2 mm and 4 mm thick panel for Loading Case PT-2,1 (with ξ_s**=0.0% and** ξ_a**=0.0%**)

Table 3.16: Comparison of average quadratic velocity of 2 mm and 4 mm thick panel for Loading Case PT-2,1 (with ξs=0.0% and ξa=0.0%)

Panel Dominated Modes						Cavity Dominated Modes				
for 2 mm thick panel			for 4 mm thick panel			Uncoupled Frequency	Coupled Case			
							for 2mm thick panel		for 4mm thick panel	
Uncoupled Freq.	Coupled Freq.	Avg. Qurd. Velocity	Uncoupled Freq.	Coupled Freq.	Avg. Qurd. Velocity		Coupled Freq.	Avg. Qurd. Velocity	Coupled Frequency	Avg. Qurd. Velocity
186.45	187	124.1	257.21	261	90.5	0.0(0,0,0)	-	-	-	-
199.08	204	100.8	321.07	321	107.6	85.02(0,0,1)	84	63.25	84	44.91
281.79	282	113.4	404.21	404	109.5	170.17(0,0,2)	164	89.79	169	65.07
292.99	293	144.7	435.75	434	104.9	255.59(0,0,3)	253	83.54	251	86.54
307.82	308	105.5				341.40(0,0,4)	338	88.24	341	69.89
373.79	374	97.4				427.74(0,0,5)	426	93.25	426	74.78
393.51	394	108.3				498.36(1,0,0)	493	96.16	489	96.87
399.13	398	110.3								
437.11	437	122.3								
463.90	458	114.4								
480.17	478	103.9								
482.13	480	98.7								

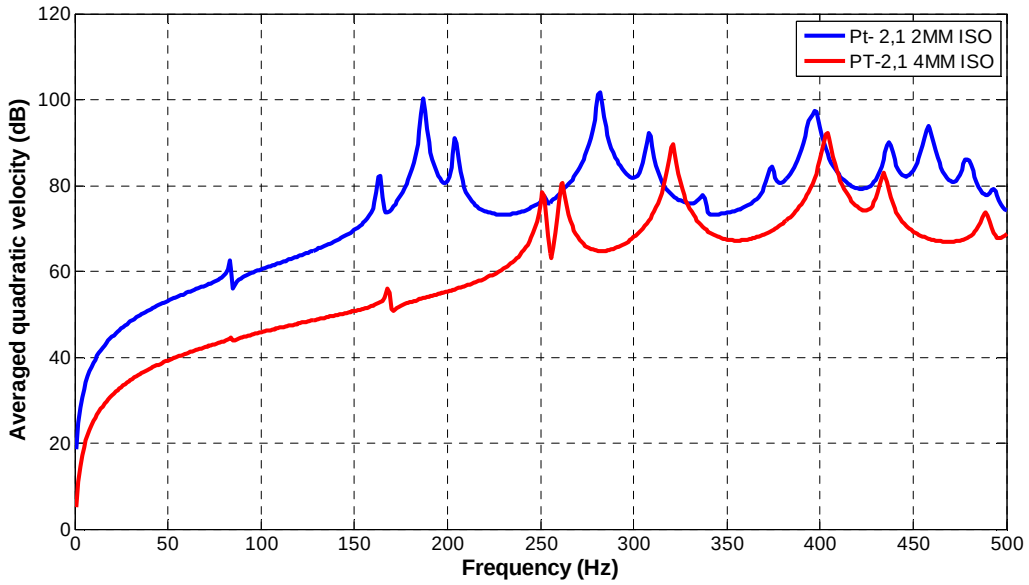

Figure 3.21: Average quadratic velocity of 2 mm and 4 mm thick panel for Loading Case PT-2,1 (with ξ_s**=0.5% and** ξ_a**=0.5%**)

Table 3.17: Comparison of average quadratic velocity of 2 mm and 4 mm thick panel for Loading Case PT-2,1 (with ξs=0.5% and ξa=0.5%)

Panel Dominated Modes						Cavity Dominated Modes				
for 2 mm thick panel			for 4 mm thick panel			Uncoupled Freq.	Coupled Case			
							for 2mm thick panel		for 4mm thick panel	
Uncoupled Freq.	Coupled Freq.	Avg. Qurd. Velocity	Uncoupled Freq.	Coupled Freq.	Avg. Qurd. Velocity		Coupled Freq.	Avg. Qurd. Velocity	Coupled Frequency	Avg. Qurd. Velocity
186.45	187	100.30	257.21	262	80.51	0.0(0,0,0)	-	-		
199.08	204	90.91	321.07	321	89.66	85.02(0,0,1)	83	62.49	84	44.73
281.79	282	101.60	404.21	404	92.31	170.17(0,0,2)	164	82.27	168	55.97
292.99	293	-	435.75	434	82.89	255.59(0,0,3)	252	77.53	251	78.45
307.82	308	92.08				341.40(0,0,4)	337	77.86	-	-
373.79	374	84.28				427.74(0,0,5)	-	-	-	-
393.51	394	-				498.36(1,0,0)	493	79.18	489	73.82
399.13	398	97.27								
437.11	437	90.17								
463.90	458	93.78								
480.17	479	86.11								
482.13										

From above some observations may be summarized as follows:

a) If the thickness increases two times, the average quadratic velocity decreases about 10-12 dB for any damping cases.
b) For cavity dominated modes, two different cases are observed. In one case (for 85.02, 170.17 and 338 Hz natural frequency) the structural velocity decreases significantly with the increase of panel thickness, indicating a weak coupling between the acoustics and structure. In another case change in structural velocity is insignificant with the increase of panel thickness, indicating the existence of a strong coupling between the acoustics and structure.

3.2.5 Case Study-4: Effect of material properties on Sound transmission

All the above studies are made on the isotropic aluminum panel. In this section, the response of structural panel made of different laminated composite material are calculated and compared with the response parameter of the isotropic aluminum panel.

The properties considered of laminated composite material considered in developed model to compute the response is listed in Table 3.18.

Table 3.18 Properties of laminated composite material considered in the present study

	Material	E11 (GPa)	E22 (GPa)	G12 (GPa)	Density (kg/m^3)	Lamina		Panel thickness
						Orientation	No. of layers	
Composite-1	High strength GR/epoxy	138	6.9	4.5	1570	30/-30 Symmetrical	4	2 mm
Composite-2	High modulus GR/epoxy	221	6.9	4.8	1600	30/-30 Symmetrical	4	2 mm
Composite-3	Ultra-high strength GR/epoxy	303	6.9	6.6	1680	30/-30 Symmetrical	4	2 mm

Using the developed model of semi-cylindrical wall panel for laminated composite material, the response of structural panel is calculated. The obtained result is compared with the response obtained from earlier model of 2mm thick panel. The PT-2,1 loading case is considered similar to earlier sub-section.

Two cases are considered, i.e. (i) structural damping 0% and acoustics damping 0% and (ii) structural damping 0% and acoustics damping 0%. Average quadratic velocity plot are for isotropic (aluminum) panel and different composite panel are given in Figure 3.22 to Figure 3.23.

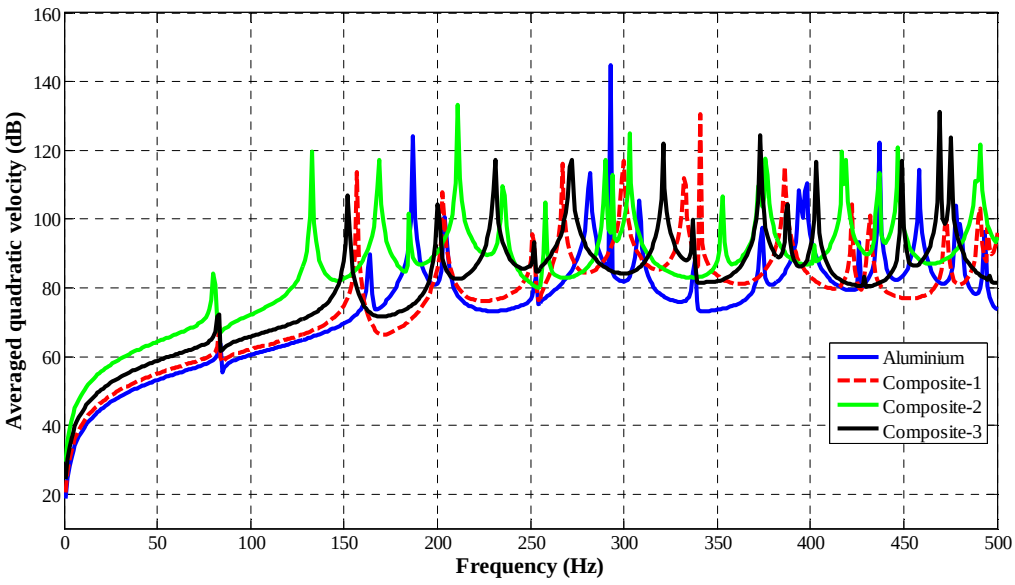

Figure 3.22: Average quadratic velocity of aluminum panel and different composite panel for Loading Case PT-2,1 (with ξ_s**=0.0% and** ξ_a**=0.0%**)

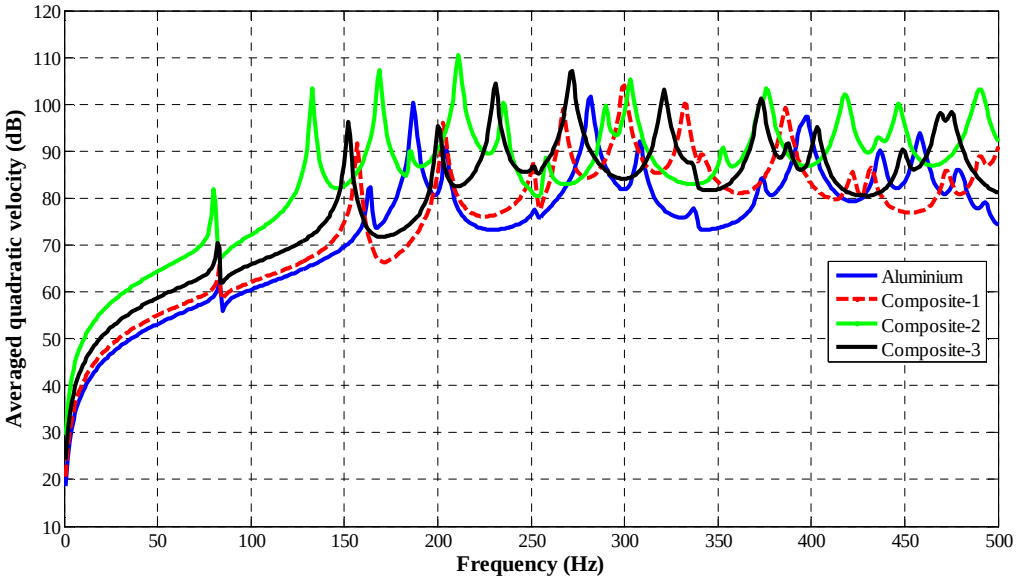

Figure 3.23: Averages quadratic velocity of aluminum panel and different composite panel for Loading Case PT-2,1 (with ξ_s**=0.5% and** ξ_a**=0.5%**)

From above some observations may be summarized as follows:

a) The energy transmission through aluminium (isotropic) panel is significantly lower than panel made of laminated composite materials for both the damping models.

b) For ξ_s**=0.0% and** ξ_a**=0.0%**, the energy transmission through composite increases with the decrease of stiffness to density ratio. The stiffness to density ratio of the materials used in modelling are listed in Table 3.19, where unit of stiffness is GPa and of density is kg/m^3.

Table 3.19 Stiffness to density ratio for different composite materials

Material	D11/ρ
Aluminium	0.019
Composite-1	0.035
Composite-2	0.054
Composite-3	0.070

3.3 Sound Transmission through Semi-cylindrical Double Wall

3.3.1 Model Properties

In the present study a Semi-cylindrical Double wall panel separated by an air gap (defined with a subscript ‘g’) is modelled. The panels are considered as simply supported along all edges. The outer panel (Panel ‘a’) is excited by Point load external excitation.

The geometric properties in different cases of Semi-cylindrical single wall panel are stated below:

i.	Length of the model (L)	:	2 m
ii.	Radius of the outer panel (R_a)	:	0.24 m
iii.	Radius of the outer panel (R_b)	:	0.2 m
iv.	The thickness of the panels	:	2 mm
v.	Thickness of air-gap	:	0.04 m ($h_e/h_g = 0.2$)
vi.	Structural Damping	:	0.0%
vii.	Acoustic Damping	:	0.0%

The panels are made of aluminium and the properties of panels and fluid in air-gap and enclosure, are considered same as for Single wall model discussed in previous sub-section. Two different damping cases are studied.

3.3.2 Effect on Sound Transmission through Double wall over Single wall panel

Till now all studies are carried out on single wall problem. In this sub-section, the response of structural panel made of double wall is calculated from developed double wall model.

The response parameter of the double wall is compared with results obtained for single wall. A point load is applied on the Panel 'a' at location z = 0.5 m and theta 67.5° (referred as PT-2,1 loading case) as shown in the Figure 3.24.

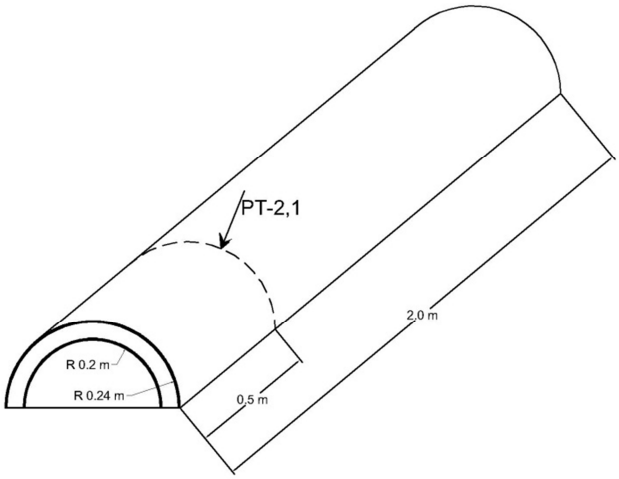

Figure 3.24: Schematic model for Semi-cylindrical single wall subject to Point Load at various loading point.

The average quadratic velocity and average sound pressure of double wall and single wall for Loading Case PT-2,1 is given in Figure 3.25 and Figure 3.26.

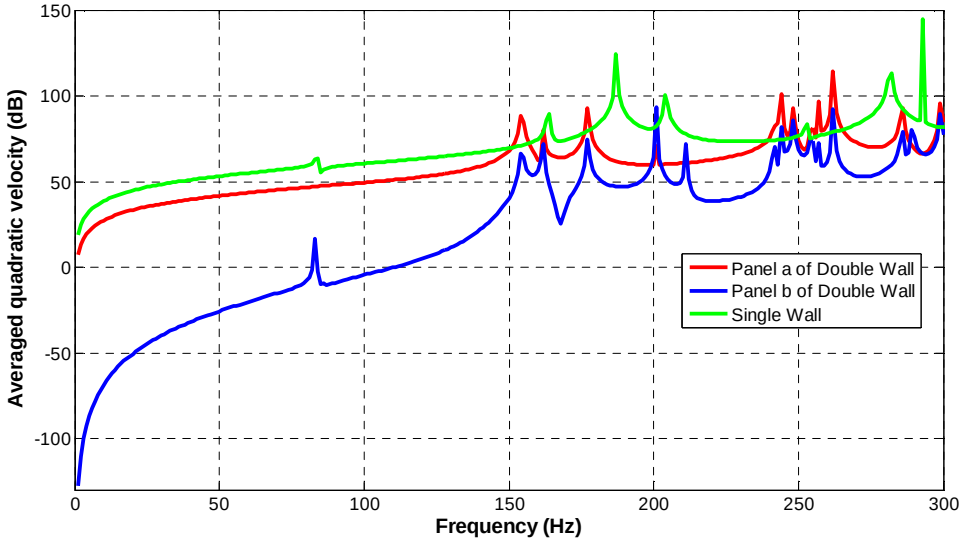

Figure 3.25: Average quadratic velocity of double wall and single wall for Loading Case PT-2,1

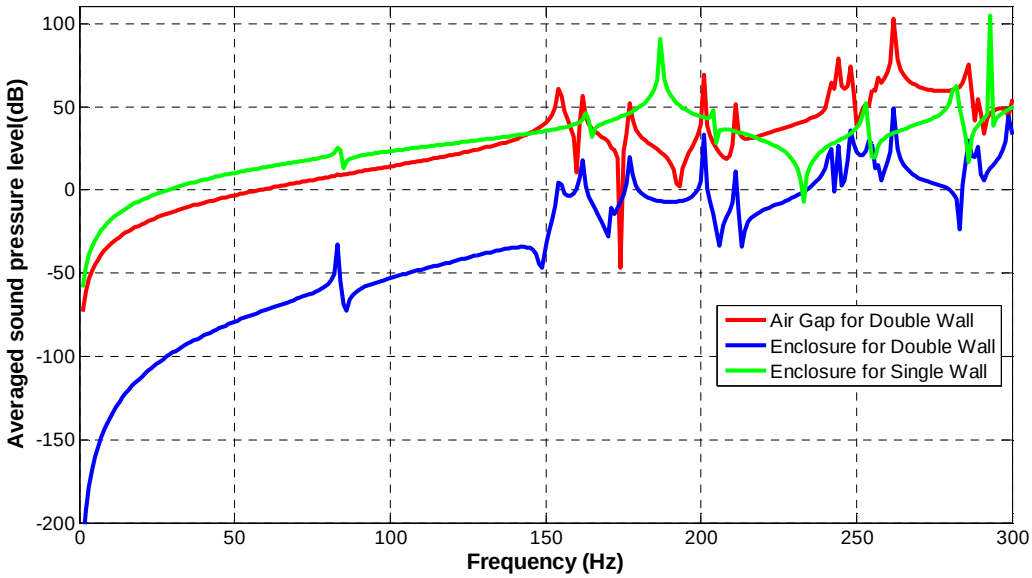

Figure 3.26: Average sound pressure of double wall and single wall for Loading Case PT-2,1

From above some observations may be summarized as follows:

a) The sound pressure level inside the enclosure is significantly lower in Single wall system than double wall system.
b) By introducing the double wall model the average sound pressure level can be reduced to 20 to 30 dB over single wall model. The reduction of sound transmission through wall is maximum for double wall model among all the cases studied in the present thesis.
c) The structural velocity of double wall panels are also significantly lower then the single wall panel, with a exception near 250 Hz frequency region. The natural frequency of the structural panels and the air-gap are closely spaced in 250 Hz frequency region, which cause a strong coupling between the structural panels and cavity domains.

CHAPTER 4: CONCLUSIONS AND FUTURE SCOPE

4.1. CONCLUDING REMARKS

A numerical model based on the finite element technique is developed in the present work to understand the sound transmission behaviour into a semi-cylindrical enclosure through the semi-cylindrical shaped flexible wall. The developed model is also extended to semi-cylindrical double wall structure separated by an air gap in between. Separate finite element models of the structural panels and the acoustic domain are developed in ANSYS (ver. 11.0) platform and a free vibration analysis is performed to get the natural frequencies and natural mode shapes. Subsequenctly, the structure and the acoustic domains are coupled using the modal expansion approach following Green's theorem to understand the energy transmission behaviour. The developed formulation is first validated for the energy transmission mechanism through a flat double wall structure with the available results from the published research article. Energy transmission characteristics through semi-cylindrical single wall structure are obtained for various loading configurations and the effects of the various damping co-efficients, thickness of panel and different material properties are studied. Transmission characteristic study through the semi-cylindrical double wall structure is also carried out. Some of the important observations that are summarized as follows:-

a. For the present semi-cylindrical single wall structure, the energy transmission characteristics are dominated primarily by the structural panel. The effect of the acoustic domain such as back pressure, on the structural panel is negligible.
b. Increase in the damping co-efficient will cause in decrease of the structural velocity significantly (Figure 3.18 to 3.19 and Table 3.13 to 3.14).
c. If the thickness of the panel of single wall structure is doubled, the average quadratic velocity decreases by 10-12 dB for any damping cases (Figure 3.20 to 3.21 and Table 3.16 to 3.17).
d. In low frequency region the performance of isotropic (aluminum) material is better than laminated composite materials in reduction of energy transmission (Figure 3.20 to 3.21).
e. The reduction of energy transmission through the panels of the double wall structure is much better than a single wall structure due to a strong back pressure effect from the air-gap separating the panels.

4.2. SCOPE FOR FUTURE WORK

Future scopes in the field related to present dissertation are enormous. Some of them are,

i) Experimental validation of coupled vibro-acoustic single and double model to estimate the energy transfer into the acoustic domain through flexible panels.

ii) Study of Sound transmission characteristics into the enclosure by incorporating the sound absorbing material layer between the panels of the double wall curved structure.

iii) In the present case sound transmission behaviour has been studied for external harmonic excitation. This work may be further extanded for other types of external excitation, viz., a turbulaent boundary layer flow over the semi-cylindrical structure to simulate a real life condition for aerospace structures.

iv) Future work can also be directed towards developing a suitable control strategy to minimize the unwanted noise transmission into the enclosure.

REFERENCES

[1] De Fonseca P., Sas P., Van Brussel H., and Henrioulle K., “Active reduction of sound transmission through double panel partitions - A physical analysis of the observed phenomena”, Proceedings of the International Conference on Noise and Vibration Engineering. International Conference on Noise and Vibration Engineering. Leuven, Belgium, Sep 13-15, 2000 (pp. 21-28).

[2] Chladni E. F. F, ‘Die Acustik’, Leipzig: Breitkopf and Hartel, (1802).

[3] Strutt John William (Lord Rayleigh), ‘The Theory of the Sound’, Macmillan and Co. Ltd., London, (1877).

[4] Lax M., "The effect of radiation on the vibration of a circular diaphragm", The Journal of Acoustical Society of America, 16 (1944) 5-13.

[5] Fay R. D., "Interaction between a plate and a sound field", The Journal of Acoustical Society of America, 20 (1948) 620-625.

[6] Finney M. J., "Reflection of sound from submerged plates", The Journal of Acoustical Society of America, 20 (1948) 626-637.

[7] Morse P. M., Ingard K. U., "Theoretical Acoustics", McGraw Hill Book Co, New York, (1968)

[8] Skudrzyk E., "The Foundations of Acoustics", Springer-Verlag, Wein, (1971)

[9] Pierce A. D., "Acoustics: An Introduction to its Physical Properties and Applications", McGraw Hill Book Co, New York, (1981)

[10] Kuttruff H., "Room Acoustics", Applied Science Publishers, London, (1973)

[11] Seto W.W., "Acoustic Theory and Problems of Acoustics, Schaum’s Outline Series", McGraw Hill Book Co, New York, (1971)

[12] Junger M. C., Feit D., "Sound, Structures, and Their Interaction", The MIT Press, (1986)

[13] Fahy Frank, Gardonio Paolo, "Sound and Structural Vibration: Radiation, Transmission and Response", Academic Press, Elsevier, Amsterdam, (2007)

[14] Norton M. P., "Fundamentals of Noise and Vibration Analysis for Engineers", Cambridge University Press, Cambridge, (1989)

[15] Beranek L. L., "Acoustic Measurements", John Wiley & Sons, Chichester, (1949)

[16] Crocker M. J., "Encyclopedia of Acoustics", John Wiley & Sons Inc, Chichester, (1997)

[17] Cremer L., “Theorie der Schälldammung dünner Wände bei Schrägen einfall”, Akust. Ztg, 7, (1942) 81-102

[18] Sharp B.H., “Prediction Methods for the Sound Transmission of Building Elements", Noise Control Engineering, 11, (1978) 63 – 63,

[19] Sewell E.C, “Transmission of reverberant sound through a single leaf partition surrounded by an infinite rigid baffle”, Journal of Sound and Vibration, 12, (1970), 21-32

[20] London A., “Transmission of reverberant sound through single walls”, The Journal of the Acoustical Society of America, 42 (1949) 605-615.

[21] Takahashi D., "Sound transmission through single plates with absorptive facings”, The Journal of the Acoustical Society of America, 83(4), (1988), 1453-1457.

[22] Takahashi D., " Sound transmission through single plates with absorptive facings: Improved theory and experiment", The Journal of the Acoustical Society of America., 88(2), (1988), 879-882.
[23] Beatty Jr., R., E., Bolt, R., H. and Young, J., 'The Transmission of sound through Single and Double Walls at Oblique Incidence', Journal of the Acoustical Society of America, Vol. 23,1951
[24] Kuroki, S. and Yasuoka, M., 'Loss Factor at the Boundary of a Single-leaf Wall under a Vibrational Field of Diffused Bending Waves', Journal of the Acoustical Society of America, Vol. 103, 1998
[25] London A., "Transmission of reverberant sound through double walls", The Journal of the Acoustical Society of America, 22 (2) (1950) 270-279.
[26] Beranek L. L., "Noise Reduction", McGraw-Hill, New York, 1960
[27] Beranek L. L., "The Forty-Fifth Thomas Hawksley Lecture: The Transmission and Radiation of Acoustic Waves by Structures", SAGE journals
[28] Cremer L. and Heckl M., "Structure-Borne Sound: Structural Vibrations and Sound Radiation at Audio Frequencies", Springer-Verlag, Berlin, (1988).
[29] K. A. Mulholland, A. J. Price and H. D. Parbrook, 'Transmission loss of Multiple Panels in a Random Incidence Field', Journal of the Acoustical Society of America, , pp. 1432-1435, 1968
[30] A. Cummings and K A. Mulholland, 'The Transmission Loss of Finite-sized Double panels in a Random Incidence Sound Field', Journal of Sound and Vibration, pp. 126-133. 1968
[31] P. H. White and A. Powell, 'Transmission of Random Sound and Vibration through a Rectangular Double Wall', Journal of the Acoustical Society of America, pp. 821-832, 1965
[32] Price, A. J. and Crocker, M. J., 'Sound Transmission through Double Panels Using Statistical Energy Analysis', Journal of Acoustical Society of America , Vol. 47, No. 3 (Part 1),1970
[33] Sas, P., Bao, C., Augusztinovicz, F., and Desmet, W., 'Active Control of Sound Transmission through a Double Panel Partition', Journal of Sound and Vibration, Vol. 180, No. 4, pp. 609 – 625, 1995
[34] Bao, C., and Pan, J., 'Experimental Study of Different Approaches for Active Control of Sound Transmission through Double Walls', Journal of Acoustical Society of America, Vol. 102, No. 3,pp. 1664 – 1670, September 1997
[35] Bao, C., and Pan, J., 'Analytical Study of Different Approaches for Active Control of Sound Transmission through Double Walls', Journal of Acoustical Society of America, Vol. 103, No. 4, pp. 1916 – 1922, April 1998
[36] Wang, J., Lu, T.J., Woodhouse, J., Langley, R.S., and Evans, J., 'Sound Transmission through Lightweight Double-Leaf Partitions: Theoretical Modelling', Journal of Sound and Vibration, Vol. 286, pp. 817 – 847, 2005
[37] Cheng, L., Li, Y. Y. and Gao, J. X., 'Energy Transmission in a Mechanically-Linked Double-Wall Structure Coupled to an Acoustic Enclosure', Journal of Acoustical Society of America, Vol. 117, No. 5, pp. 2742 – 2751, 2005

[38] Li, Y. Y and Cheng, L., ‘Active Noise Control of a Mechanically Linked Double Panel System Coupled with an Acoustic Enclosure’, Journal of Sound and Vibration, Vol. 297, pp. 1068 – 1074, 2006
[39] Smith P.W., “Sound transmission through thin cylindrical shells”, The Journal of the Acoustical Society of America, 29 (6) (1957) 721-729
[40] Koval L.R., “On sound transmission into a thin cylindrical shell under Flight Conditions”, Journal of Sound and Vibration, 48 (2) (1976) 265-275.
[41] Koval L.R., “Effects of cavity resonances on sound transmission into a thin cylindrical shell”, Journal of Sound and Vibration, 59 (1) (1978) 23-33.
[42] Koval L.R., “On sound transmission into a stiffened cylindrical shell with rings and stringers treated as discrete elements”, Journal of Sound and Vibration, 71 (4) (1980) 511-521.
[43] Blaise A., Lesueur C., Gotteland M. And Barbe M. ,”On sound transmission into an orthotropic infinite shell: comparison with Koval’s results and understanding of phenomena”, Journal of Sound and Vibration (1991) 150(2), 233-243
[44] Daneshjou K., Nouri A. and Talebitooti R., “Sound transmission through laminated composite cylindrical shells using analytical model”, Archive of Applied Mechanics, 77 (2007) 363-379.
[45] Bilong Liu, Leping Feng, Anders Nilsson, “Sound transmission through curved aircraft panels with stringer and ring frame attachments”, Journal of Sound and Vibration 300 (2007) 949–973
[46] Chang M. T. And Vaicaitis R., “Noise transmission into semi-cylindrical enclosures through discretely stiffened curved panels”, Journal of Sound and Vibration (1982) 85(l), 71-83